NASA TECHNICAL MEMORANDUM

NASA TM X–62,058

NASA TM X–62,058

AERODYNAMIC HEATING OF A SPACE SHUTTLE DELTA–WING BOOSTER AT $M_\infty = 7.4$

Charles E. DeRose and William K. Lockman

Ames Research Center
Moffett Field, Calif. 94035

August 1971

AERODYNAMIC HEATING OF A SPACE SHUTTLE DELTA-WING BOOSTER AT $M_\infty = 7.4$

by

Charles E. DeRose and William K. Lockman

ABSTRACT

An experimental investigation was performed to obtain detailed aerodynamic heating distributions on a model of a space shuttle delta-wing booster. Test results were obtained for an angle-of-attack range from -5° to 60° at a free-stream Mach number of 7.4 and free-stream Reynolds numbers, based on model reference length (distance from nose to base of delta wing), from 1 to 5 million. Results showing the effect of Reynolds number and vehicle attitude on the vehicle heating are presented and discussed.

AERODYNAMIC HEATING OF A SPACE SHUTTLE DELTA-WING BOOSTER AT $M_\infty = 7.4$

by

Charles E. DeRose and William K. Lockman

SUMMARY

An experimental investigation has been conducted in the Ames' 3.5-foot hypersonic wind tunnel at a Mach number 7.4, to determine the heating rate distribution on a space shuttle delta-wing booster. The model, instrumented with thermocouples, was a 0.006 scale version of the General Dynamics/Convair Corporation B-9J delta-wing booster. The test covered a range of Reynolds numbers (based on model length and free-stream conditions) from 1 to 5 million and angles of attack from -5° to 60°. Tabulated test results for the complete test program are included. Representative plotted results showing the effects of Reynolds number and vehicle attitude (angle of attack) on the vehicle heating distributions are presented and discussed.

INTRODUCTION

The NASA is currently investigating the concept of a fully reusable, two-stage space shuttle system to transport payloads from earth to low-earth orbit and return (see ref. 1). The first stage of such a shuttle system is a booster that will provide the initial acceleration, and the second stage is an orbiter, containing the payload, that will continue into orbit. Both of these stages must be capable of returning to the launch site, or other predetermined locations, and making conventional airplane-type landings.

Successful development of such a space shuttle system will require the understanding of problems in many technological areas. In particular, to be entirely reusable, these vehicles must be designed to withstand the heating encountered during their flights without structural damage. This requires the accurate mapping of the heating rate inputs for the proposed configurations and flight trajectories so that precise heat protection structures can be designed.

The present experimental investigation was performed in a manner to obtain detailed aerodynamic heating distributions on a delta-wing booster model for a range of test conditions. The test model, instrumented with thermocouples, was provided by General Dynamics/Convair Corporation (GD/C) and was a 0.006 scale representation of the GD/C B-9J delta-wing booster. The test program was conducted in the Ames' 3.5-foot hypersonic wing tunnel for an angle-of-attack range from -5° to 60° at a free-stream Mach number of 7.4 and free-stream Reynolds numbers, based on model length, from 1 to 5 million. Results showing the effects of Reynolds number and angle of attack on the vehicle heating distributions are presented in both tabular and graphical form.

The authors gratefully acknowledge the help of Andre Roberge and Nick Nicodemius from General Dynamics/Convair Corporation in the performance of this tunnel test program.

NOMENCLATURE

c	specific heat of model skin material
L	model reference length
M_∞	free-stream Mach number
$\dot{q}$	heat transfer rate
$\dot{q}_s$	stagnation-point heat transfer rate for reference sphere
$\dot{q}_w$	heat transfer rate at model wall
R_s	reference sphere radius equivalent to 0.305 m (1 ft) at model scale
$Re_{\infty,L}$	free-stream Reynolds number based on model reference length, L
T_w	temperature, at model wall
t	time
x	body axial distance from nose
α	angle of attack
ϕ	body circumferential angle (positive measured clockwise from bottom centerline as viewed from rear of model)
ρ	density of model skin material
τ	thickness of model skin

EXPERIMENTAL METHOD

Facility

The test program was conducted in air in the Ames' 3.5-foot hypersonic wind tunnel. This facility, described in reference 2, is a blow-down-type tunnel with a pebble-bed heater to heat the air and axisymmetric contoured nozzles to provide flow Mach numbers of 5.2, 7.4, and 10.4. The nozzle walls are film-cooled by helium injected into the nozzle boundary layer through slots upstream of the throat. The tunnel is equipped with a model quick-insert mechanism for quickly moving models into and out of the airstream.

A high-speed analog-to-digital data acquisition system is used for recording test data on magnetic tape. The present system is equipped to receive the electrical signals from 80 thermocouples and/or other types of transducers in addition to 20 channels reserved for tunnel parameters.

Model

The test model, provided by General Dynamics/Convair Corporation (GD/C), was a 0.006 scale representation of the GD/C B-9J delta-wing booster. The dimensions and specifications for this model and for the full-scale vehicle are given in tables (supplied by General Dynamics/Convair Corporation) listed in Appendix A. A photograph of the model is displayed in figure 1, and a three-view drawing showing the principal dimensions is given in figure 2.

The basic model geometry consisted of a fuselage body (B_7), a delta-wing (W_5), and a vertical tail (V_3). The model was constructed of 17-4 PH

stainless steel with the instrumented areas machined to a nominal skin thickness of 1 millimeter (0.040 in.) on the body and 0.5 mm (0.020 in.) on the wing and tail. The actual skin thickness was measured at each instrumented location using micrometers. Model instrumentation consisted of 100 iron-constantan thermocouples (30 gage wire) spot-welded to the inner surface of the model at the locations listed in table I and shown sketched in figure 3. For this test program, the 80 thermocouples (T/C) listed in table II were connected to the data acquisition system.

Test Conditions

As shown by the run schedule in table III, this test program was conducted at a free-stream Mach number of 7.4 for a range of free-stream Reynolds numbers, based on model length (reference length is measured from model nose to base of delta wing (see fig. 2)), between 1 and 5 million. Data were obtained for the angle of attack, α, range from -5° to 60°, with particular emphasis on values of 0°, 30°, and 60°. The runs made at α = -5° along with those at 0°, provide booster-alone data as baseline information for another test program with the orbiter mated to a booster as a launch configuration.

The specific test conditions, including the tunnel free-stream total temperature and pressure, are given for each run in Appendix B. For convenience, the tabulated data are arranged in the order of the run schedule given in table III.

Test Procedures and Data Reduction

The model with a base sting was mounted at a preset attitude on a quick-insert mechanism. This mechanism injected the model into the airstream when steady-state test conditions were established and retracted the model at the completion of data acquisition. The model injection and retraction times were each set at about 1/2 second and the time on the tunnel centerline was set at about 1 second.

The model wall temperature data for each thermocouple location and the tunnel conditions were recorded on magnetic tape at 0.07-second intervals during the test, with the data acquisition starting with the first motion of the quick-insert strut. The measured wall temperatures were differentiated with respect to time on a digital computer and the wall heat-transfer rate, $\dot{q}_w$, was then determined by the thin-skin technique using the following relationship

$$\dot{q}_w = \rho c \tau \frac{dT_w}{dt} \tag{1}$$

The data reduction program yields, for each thermocouple location, tabulated and plotted outputs of both wall temperature and heat transfer rate versus time. Lateral and longitudinal heat-conduction errors in the model skin at any given location were minimized by using the data obtained at the earliest possible time after the model cleared the tunnel boundary layer when temperatures over the surface were still close to uniform. This minimum time was influenced primarily by the combined effects of the model material response time (about 0.1 sec) and the model transit time (dependent upon model attitude)

through the tunnel boundary layer. As would be expected, heat-conduction effects were generally limited to regions with small radii of curvature where large temperature gradients were present, namely, the fuselage nose and wing and tail leading edges.

To normalize the measured heating rates, the data were divided by the theoretical stagnation-point heating rate for a sphere (ref. 3), $\dot{q}_s$, with a radius equivalent to 0.305 meter (1 ft) on the full-scale vehicle. This value of $\dot{q}_s$ was evaluated for each run (listings in Appendix B) using the measured wind tunnel conditions. The wall temperature used for the calculation of $\dot{q}_s$ was taken for a fuselage nose thermocouple when the model reached the tunnel centerline. Therefore, the sphere wall temperature was generally higher than the model temperatures determined at the earlier times when the model heating rates were evaluated. Therefore, the higher reference sphere temperature would give a relatively smaller value of $\dot{q}_s$, and thus produce a slightly larger, or more conservative, value for the heating rate ratio $\dot{q}_w/\dot{q}_s$. However, this effect is small, usually less than 10 percent of the calculated value and probably within the experimental accuracy. As an estimate, the maximum error in heating rate ratio, $\dot{q}_w/\dot{q}_s$, is ±10 percent for $\dot{q}_w/\dot{q}_s \geq 0.01$ and ±0.002 for $\dot{q}_w/\dot{q}_s < 0.01$.

The calculation of both the reference sphere heating and the Reynolds number included the use of Keyes' equation for viscosity (ref. 4) and the corrections in reference 5 for calorically imperfect, thermally perfect gas.

The theoretical values of laminar heat transfer rates, which are used as comparisons to the experimental data, were obtained using infinite swept-cylinder theory (refs. 6 and 7) modified to account for the difference in

crossflow velocity gradient between the actual body and a cylinder. A discussion of this method for a similar application can be found in reference 8.

RESULTS AND DISCUSSION

Complete results for every run of this test program are shown in tabular form in Appendix B in the order of the run schedule given in table III. For each run, these results include both the wall temperature, T_w, and the heat rate ratio, $\dot{q}_w/\dot{q}_s$, for each specified thermocouple location on the model and the particular test conditions for the run.

Representative heating rate distributions for the body, wing, and tail are shown in graphical form as plotted in figures 4 to 19. These results are mainly concerned with tests made at angles of attack of 0°, 30°, and 60°, angles which were considered most important relative to the vehicle's anticipated flight trajectory.

Body

Body heating data for the bottom centerline, the top centerline, and for various body cross sections are presented in figures 4 and 5, 7, and 8 to 10, respectively.

Bottom centerline.- Heating rates for the bottom centerline of the body at $\alpha = 0°$, 30°, and 60°, are plotted in figure 4 for Reynolds numbers from approximately 1 to 5 million. As shown, the heating rate ratios are little affected by changes in Reynolds number. However, the data for the highest Reynolds number at $\alpha = 60°$ beyond $x/L = 0.65$ show an increase in heating with an increase in Reynolds number, indicating that transition to turbulent

boundary layer flow occurs. The heating rates measured are a function of the body bottom centerline contour. The heating rate decreases with distance back from the nose until reaching the start of the first ramp (x/L = 0.39). Here, the heating rate rises slightly and continues almost level until the beginning of the flat portion of the body (x/L = 0.65). After this point, the heating rate generally decreases except for the high Reynolds number results at $\alpha = 60°$. Predictions of the laminar heating rates using modified swept-cylinder theory are shown for locations ahead of the wing for angles of attack of 30° and 60°. The predicted values agree quite well with the data except for the nose region where the two-dimensional theory underpredicts the heating of the three-dimensional stagnation region.

While the results at the above three angles of attack appear fairly normal, an unusual effect is noted at intermediate angles of attack. Figure 5 shows heating rate ratios for the bottom centerline at a nominal Reynolds number of 5 million for angles of attack of 0°, 10°, 20°, 30°, 40°, 50°, and 60°. For all angles of attack, the heating rates show a consistent pattern back to x/L = 0.39 (the start of the first ramp, as is indicated in the sketch at the top of the figure). Beyond this point, the heating rates for angles of attack of 40° and 50° depart markedly from the remainder of the data. This large increase in heating rate for these two angles of attack suggest boundary layer transition from laminar to turbulent flow occurs, probably triggered by the abrupt body contour change. Figure 6 shows a shadowgraph of this model at Mach number 7.5 and Reynolds number 6.4×10^6 at an angle of attack of 40°. A strong shock wave can be seen originating at the beginning of the front ramp and the flow aft of the shock wave appears to be turbulent. At this time, it is not clear why this effect is noted only at angles of attack of 40° and 50°.

Top centerline.- The effects of Reynolds number on leeward heating for various angles of attack along the top centerline of the body are shown in figure 7. The major items of interest for these data are the high heating rates measured for the front face of the canopy and their sensitivity to changes in Reynolds number. At all three angles of attack, 0°, 30°, and 60°, the heating rates on the canopy vary directly with Reynolds number, and their highest values are some six to seven times that measured at other points on the top centerline. It is also interesting to note that the heating rates measured on the canopy face are somewhat higher at 60° than those measured at 30°. The remainder of the data measured on the top centerline is relatively unaffected by Reynolds number and generally shows a decrease in heating with increasing angle of attack.

Cross sections.- Heating distributions for seven body cross sections are plotted in figures 8, 9, and 10, for angles of attack of 0°, 30°, and 60°, respectively. The data are plotted against ϕ around the body from the bottom centerline ($\phi = 0°$) to the top centerline ($\phi = 180°$). The first five cross-section locations are ahead of the wing and the last two are aft of the wing-body junction.

At 0° angle of attack the cross-section heating rates indicate little effect of Reynolds number except for $x/L = 0.108$, $\phi = 135°$. This location (see the thermocouple's location in fig. 3(c)) is on the side of the canopy and the data reflect the large effect of Reynolds number in the canopy region, as noted in the discussion of figure 7(a).

Figures 9 and 10, angles of attack of 30° and 60°, respectively, show no effect of Reynolds number and serve mainly to indicate the large change

in heating from windward to leeward surfaces. However, it is interesting to note that the chine heating rate (for example at $x/L = 0.346$) can exceed the heating rate on the bottom surface.

Wing

Wing heating data for the leading edge, bottom, and top surfaces are presented in figures 11, 12 to 15, and 16, respectively.

Leading edge.- Spanwise heating distributions on the wing leading edge are given in figure 11 for angles of attack of 0°, 30°, and 60°. There is practically no effect of Reynolds number on the results shown. The important result shown here is that the absolute level of heating rates is not excessively high. As an example, a heating rate ratio of 0.3 represents a radiatively cooled surface temperature of about 1400° K (2000° F), assuming $\dot{q}_s = 50$ Btu/ft^2/sec and a surface emissivity of 0.8. Thus it is seen that the temperatures that these heating rates produce can be tolerated with present day materials and technology.

Bottom surface.- Spanwise heating distributions on the wing bottom surface are shown in figure 12 for 10 percent chord, figure 13 for 50 percent chord, and in figure 14 for 75 percent chord. The data at 10 percent chord show no effect of Reynolds number, though admittedly, the heating distribution is not well defined because only two thermocouples are available. At 50 percent chord, a strong effect of Reynolds number is evident inboard at $\alpha = 30°$ and outboard at $\alpha = 60°$. In fact, the heating rate at the high Reynolds number at $\alpha = 60°$ exceeds that measured for the leading edge. The same trends that were shown at 50 percent chord also occur at 75 percent chord (fig. 14) and in addition the inboard heating rates at $\alpha = 60°$ are also a function of Reynolds number.

Figure 15 displays the effect of angle of attack on the chordwise heating of the bottom surface of the wing for two span locations, 15.7 percent and 50 percent of the exposed semispan, for a nominal Reynolds number of 5 million. At 15.7 percent of the exposed semispan (fig. 15(a)), the heating rates for angles of attack of 0°, 10°, and 20° are fairly well ordered; high heating at the leading edge, then decreasing values with increasing chord position, and then (except for 0°) increased heating toward the trailing edge of the wing. However, for α = 30° and 40°, the heating rate rises abruptly beyond the 30 percent chord point. At 50° angle of attack, the heating rate rises just behind the leading edge and stays fairly level back over the wing. These three results indicate various lengths of turbulent boundary layer flow and are probably connected with the transition noted on the body bottom centerline at 40° and 50° angle of attack. At 60° angle of attack, the heating rate for the wing bottom surface has dropped back down, again following the example of what occurred on the bottom centerline of the body. Note, the lines connecting the data points on this plot are intended to merely join the points for ease of viewing; they cannot be taken as definitive interpolations of the measured points.

The data for 50 percent exposed semispan (fig. 15(b)) present much the same picture as figure 15(a), except that the break in trend does not occur until α = 40°, and that the heating rates at lower angles do not rise toward the trailing edge of the wing.

Top surface.- Figure 16 shows the spanwise heating rate distribution for the top surface of the wing at 10 percent chord. There is practically no effect of Reynolds number on these data. The level of the heating data

shows that the top surface of the wing is effectively shielded from the flow at angles of attack of 30° and 60°. The data at $\alpha = 60°$ show very small heating, and are almost at the accuracy limit of the test.

Tail

The heating rates measured for the vertical tail are shown in figures 17, 18, and 19, for angles of attack of 0°, 30°, and 60°, respectively. All figures plot chordwise heating rates for three tail height positions, 10 percent, 50 percent, and 75 percent of the exposed height.

Figure 17 for $\alpha = 0°$, shows the high heating at the leading edge (almost constant for all height positions) followed by an immediate drop off to low heating rates over the remainder of the tail. There is little effect of Reynolds number on these heating rates, the only variation showing up at 10 percent height at the leading edge, where body-tail interference could be affecting the data.

At 30° angle of attack (fig. 18) the level of tail heating is down by a factor of ten from that at 0°. However, the trends are still the same, highest heating at the leading edge and dropping off immediately. There is a variation of heating rate with Reynolds number at the leading edge which occurs at all height positions at this angle of attack. Note, there is a random rather than systematic variation of heating rate with Reynolds number.

At 60° angle of attack (fig. 19), the heating rates are seen to be directly a function of Reynolds number at all points and the leading edge is no longer the highest heating point. The tail is in a largely separated

flow region and these results suggest that its nature is a strong function of Reynolds number.

CONCLUDING REMARKS

Heating rate distributions over the body, wing, and vertical tail of a space shuttle, delta-wing booster have been measured at a Mach number of 7.4 and Reynolds numbers from 1 to 5 million. The following results are indicated.

1. Heating rates on the windward side of the body are largely laminar and well predicted by swept-cylinder theory (ahead of the wing) up to an angle of attack of 30°. Transition to turbulent flow occurred for angles of attack of 40° and 50°, starting at the beginning of a ramp ($x/L = 0.39$). At 60° angle of attack, the heating rates indicated laminar flow until $x/L = 0.65$.

2. Heating rates on the leeward side of the body were characteristically low except for those on the canopy face. Here, high heating rates, which varied with Reynolds number, were measured for all angles of attack.

3. Transition of the boundary layer flow from laminar to turbulent appeared to occur on the wing lower surface for angles of attack of 30° to 50° as evidenced by increases in the heating rate. This effect was probably connected with the boundary layer transition on the body bottom centerline.

REFERENCES

1. Tischler, A. O.: Defining a Giant Step in Space Transportation. Astron. and Aeron., vol. 9, no. 2, Feb. 1971, pp. 22-25.

2. Holdaway, G. H.; Polek, T. E.; and Kemp, J. H., Jr.: Aerodynamic Characteristics of a Blunt Half-Cone Entry Configuration at Mach Numbers of 5.2, 7.4, and 10.4. NASA TM X-782, 1963.

3. Fay, J. A.; and Riddell, F. R.: Theory of Stagnation Point Heat Transfer in Dissociated Air. J. Aeron. Sci., vol. 25, no. 1, Feb. 1958, pp. 73-85.

4. Bertram, M. H.: Comment on "Viscosity of Air." J. Spacecraft Rockets, vol. 4, no. 2, Feb. 1967, pp. 287-288.

5. Ames Research Staff: Equations, Tables, and Charts for Compressible Flow. NACA Report 1135, 1953.

6. Beckwith, I. E.; and Cohen, N. B.: Application of Similar Solutions to Calculation of Laminar Heat Transfer on Bodies with Yaw and Large Pressure Gradient in High-Speed Flow. NASA TN D-625, 1961.

7. Beckwith, I. E.; and Gallagher, J. J.: Local Heat Transfer and Recovery Temperatures on a Yawed Cylinder at a Mach Number of 4.15 and High Reynolds Numbers. NASA TR R-104, 1961.

8. Lockman, W. K.; and DeRose, C. E.: Aerodynamic Heating of a Space Shuttle Delta-Wing Orbiter, NASA TM X-62,057, 1971.

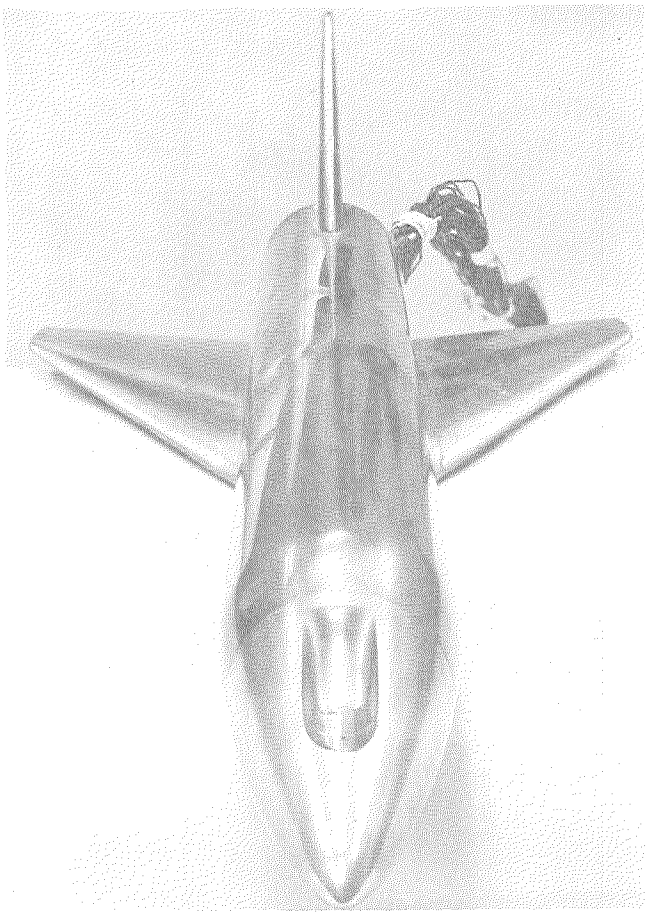

(a) Top forward view.

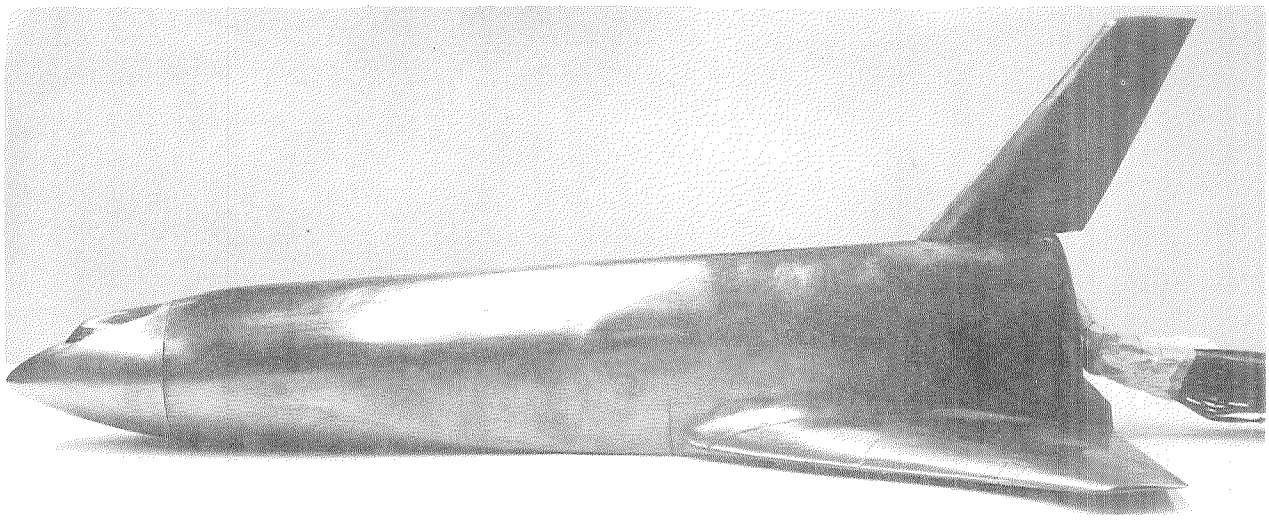

(b) Side view.

Figure 1.- Photographs of delta-wing booster model.

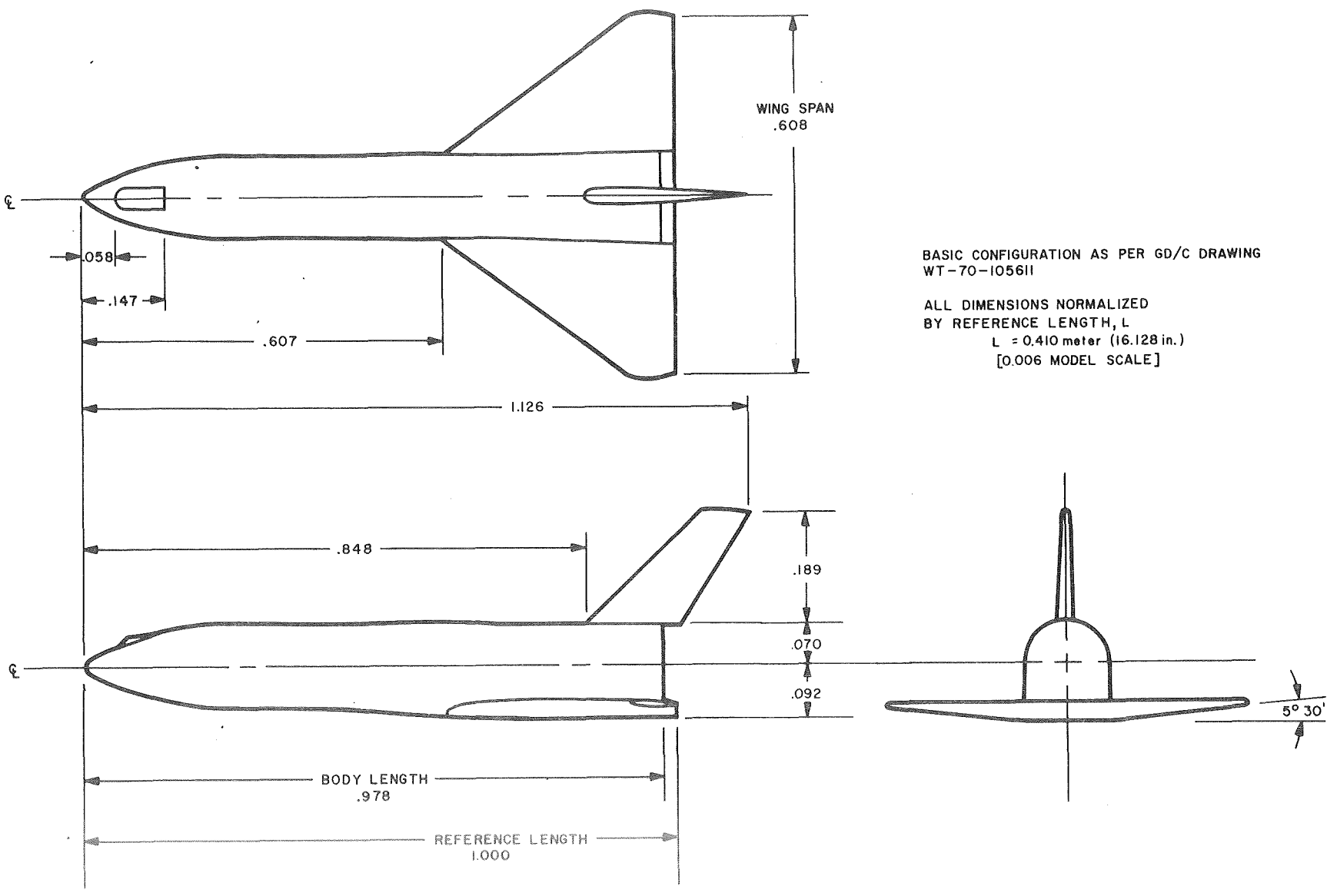

Figure 2.- Dimensioned sketch of delta-wing booster model.

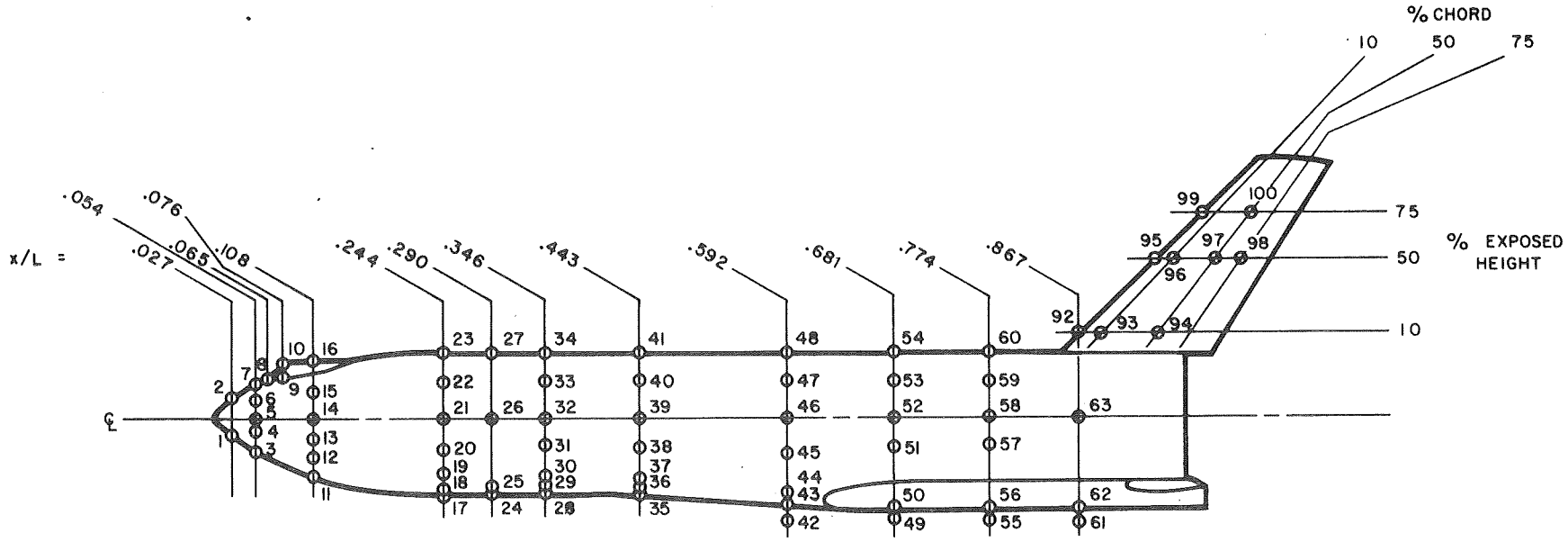

(a) Body and vertical tail.

Figure 3.- Thermocouple locations on delta-wing booster model.

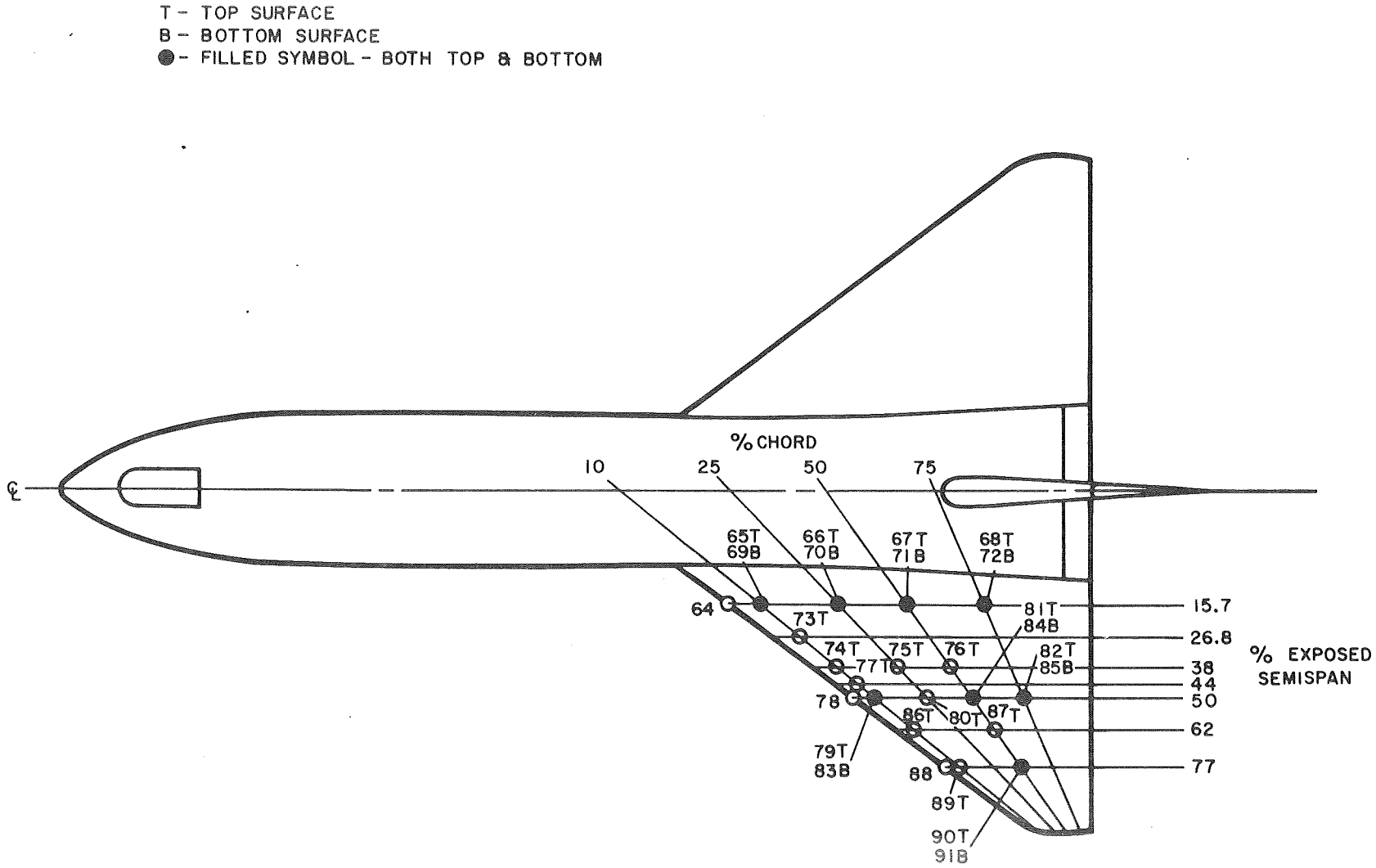

(b) Wing.

Figure 3.- Continued.

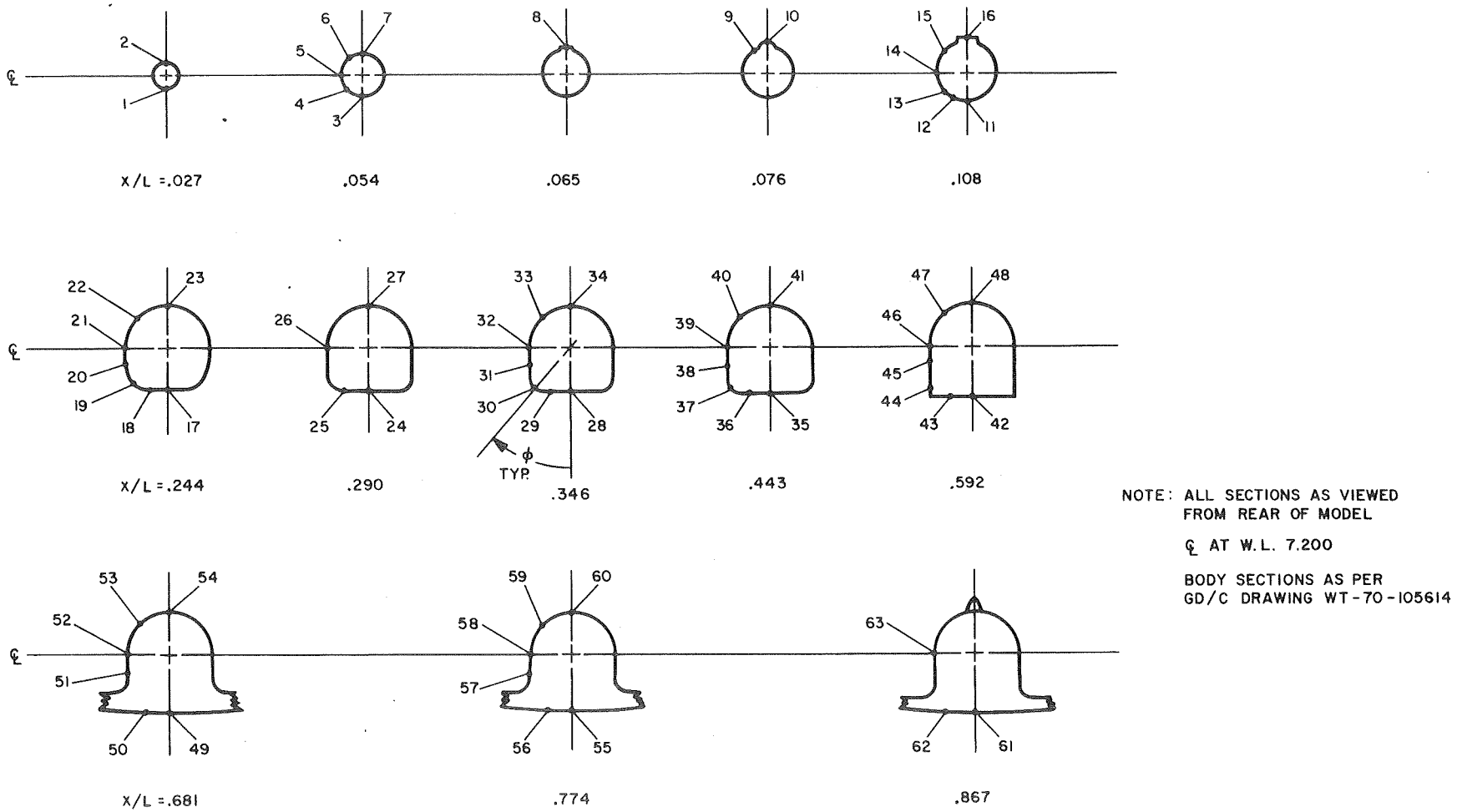

(c) Body cross sections.

Figure 3.- Concluded.

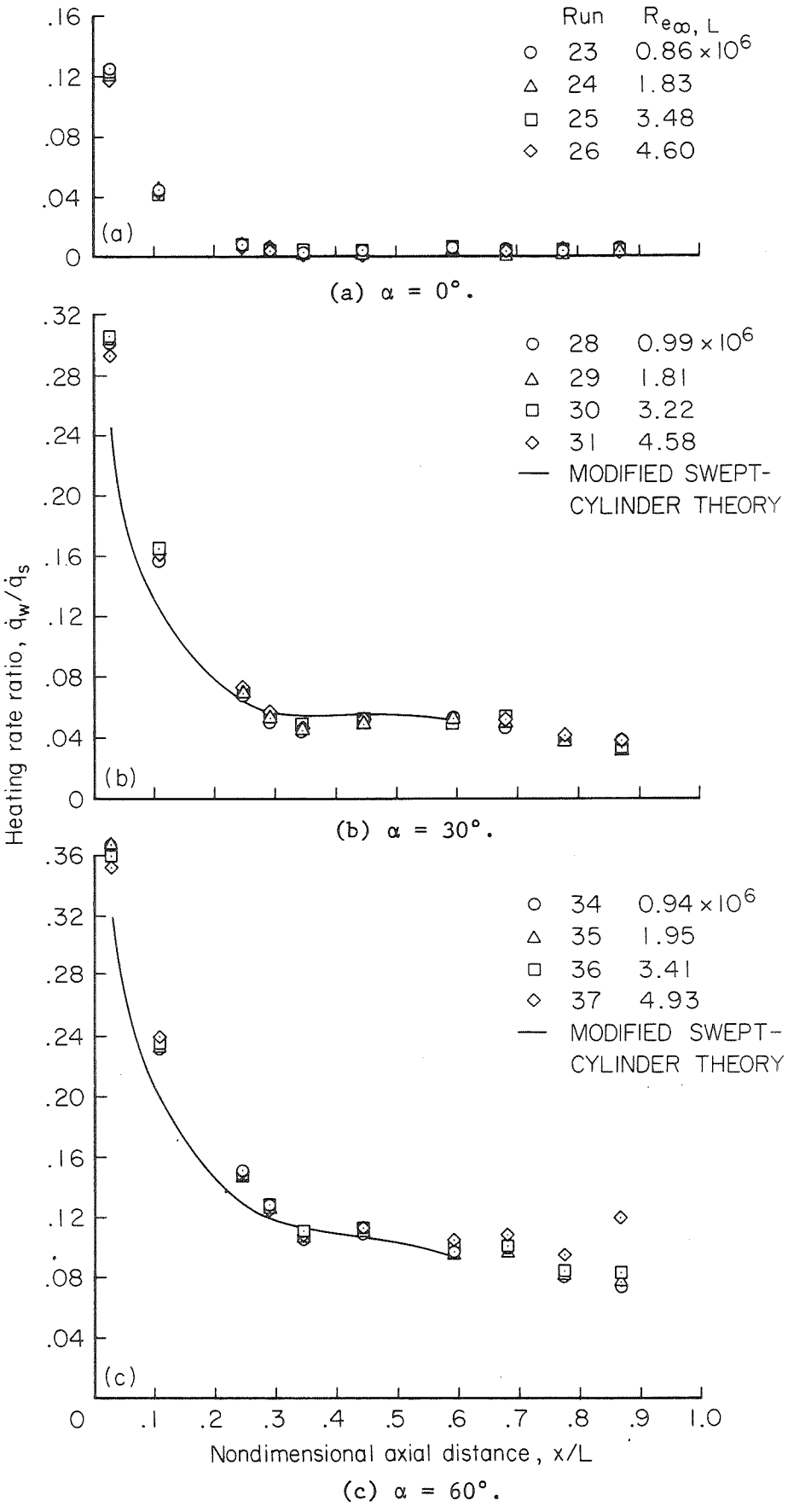

Figure 4.- Effect of Reynolds number on body bottom centerline heating rates.

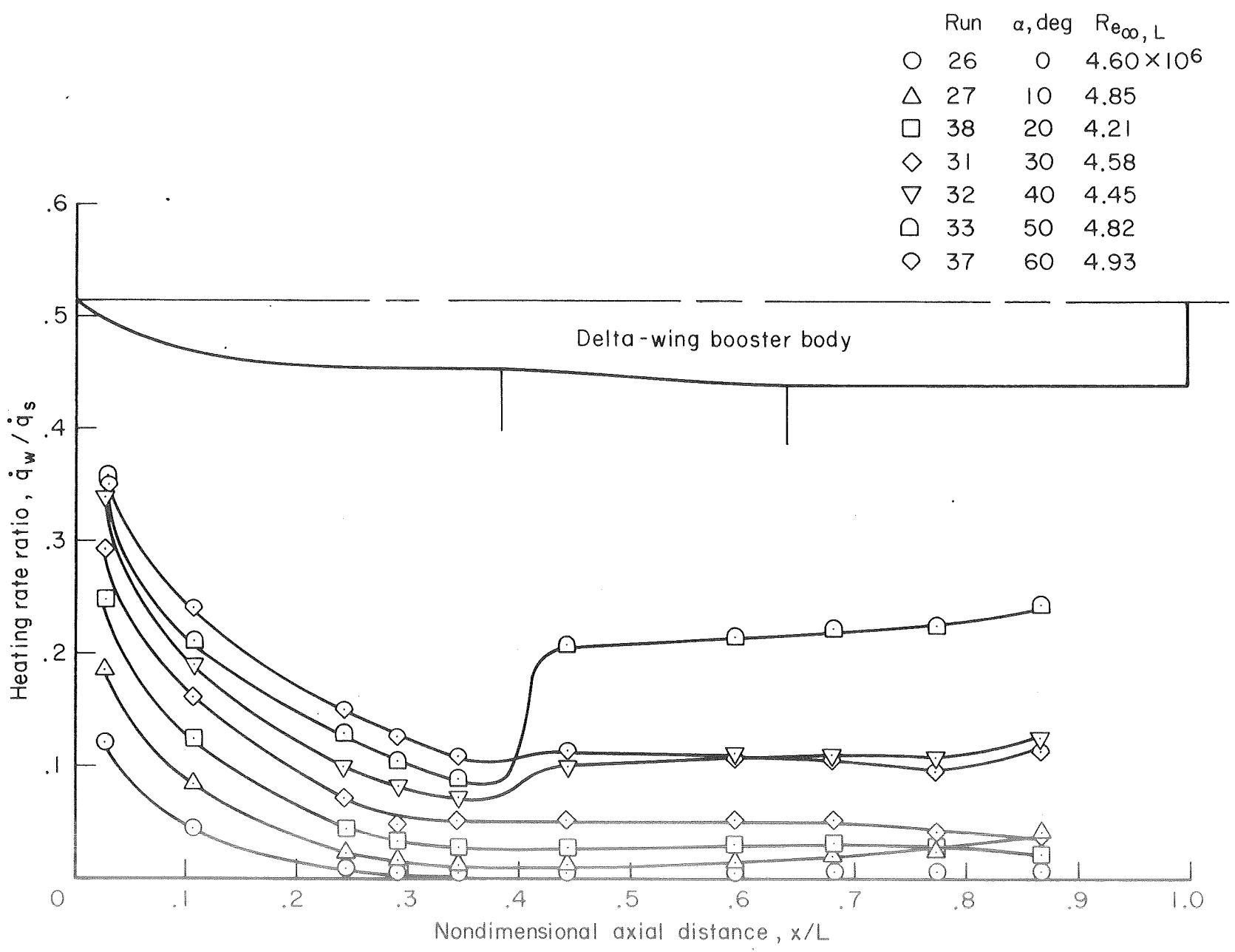

Figure 5.- Effect of angle of attack on body bottom centerline heating rates; $Re_{\infty,L} \approx 5$ million.

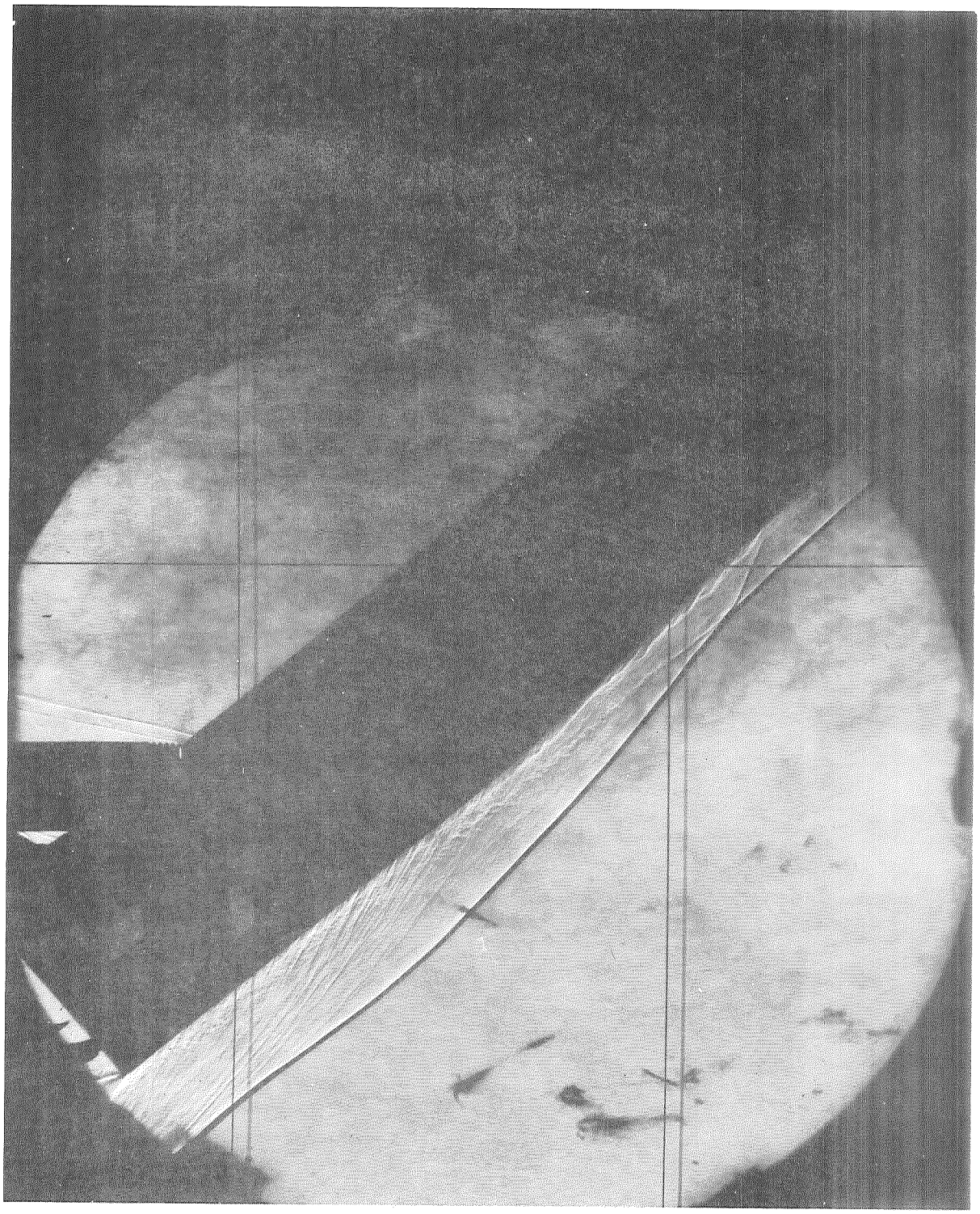

Figure 6.- Shadowgraph of delta-wing booster model; $M_\infty = 7.5$; $Re_{\infty,L} = 6.4 \times 10^6$; $\alpha = 40°$.

(Shadowgraph taken in Ames Hypervelocity Free-Flight Facility.)

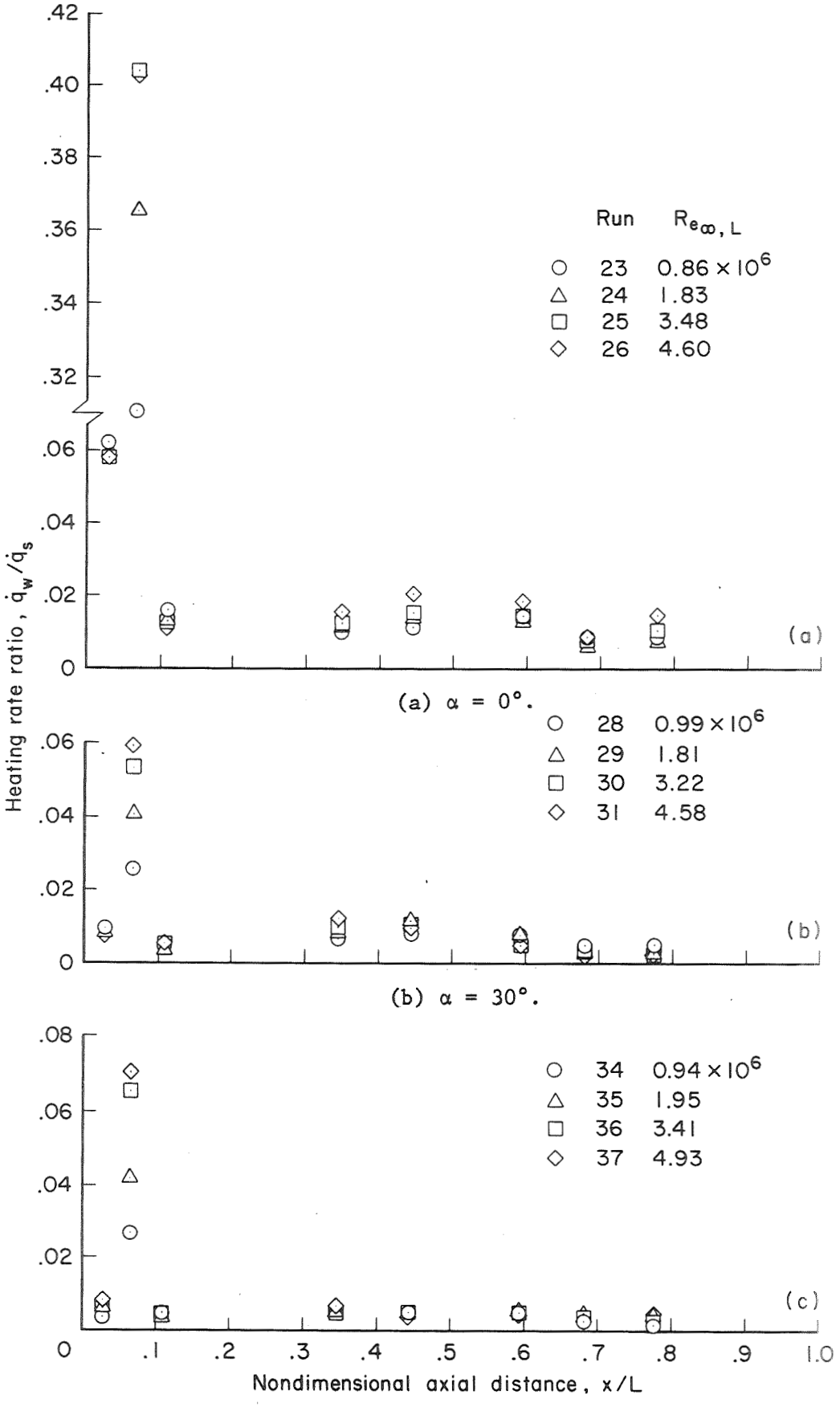

Figure 7.- Effect of Reynolds number on body top centerline heating rates.

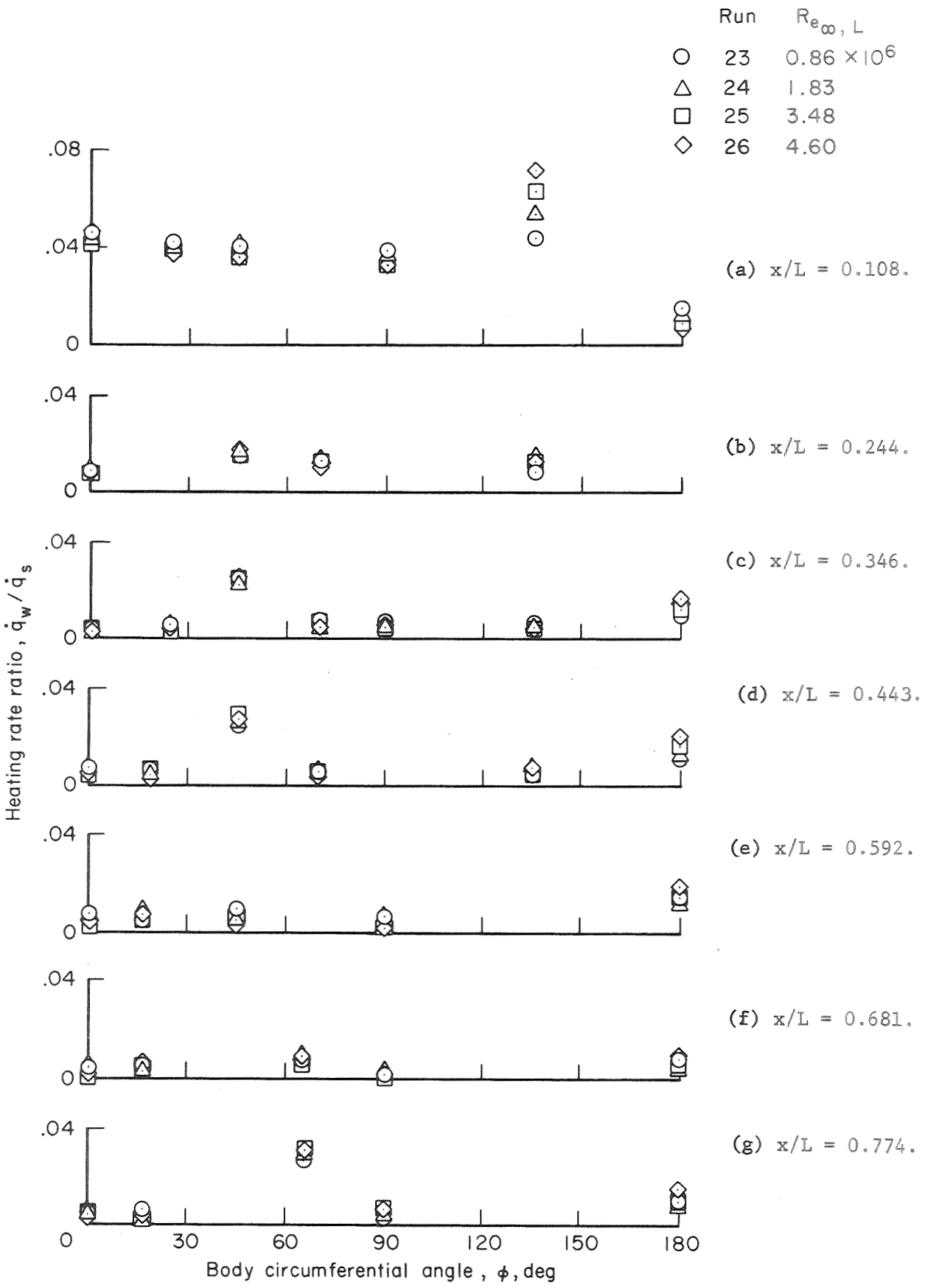

Figure 8.- Body cross-section heating rates; $\alpha = 0°$.

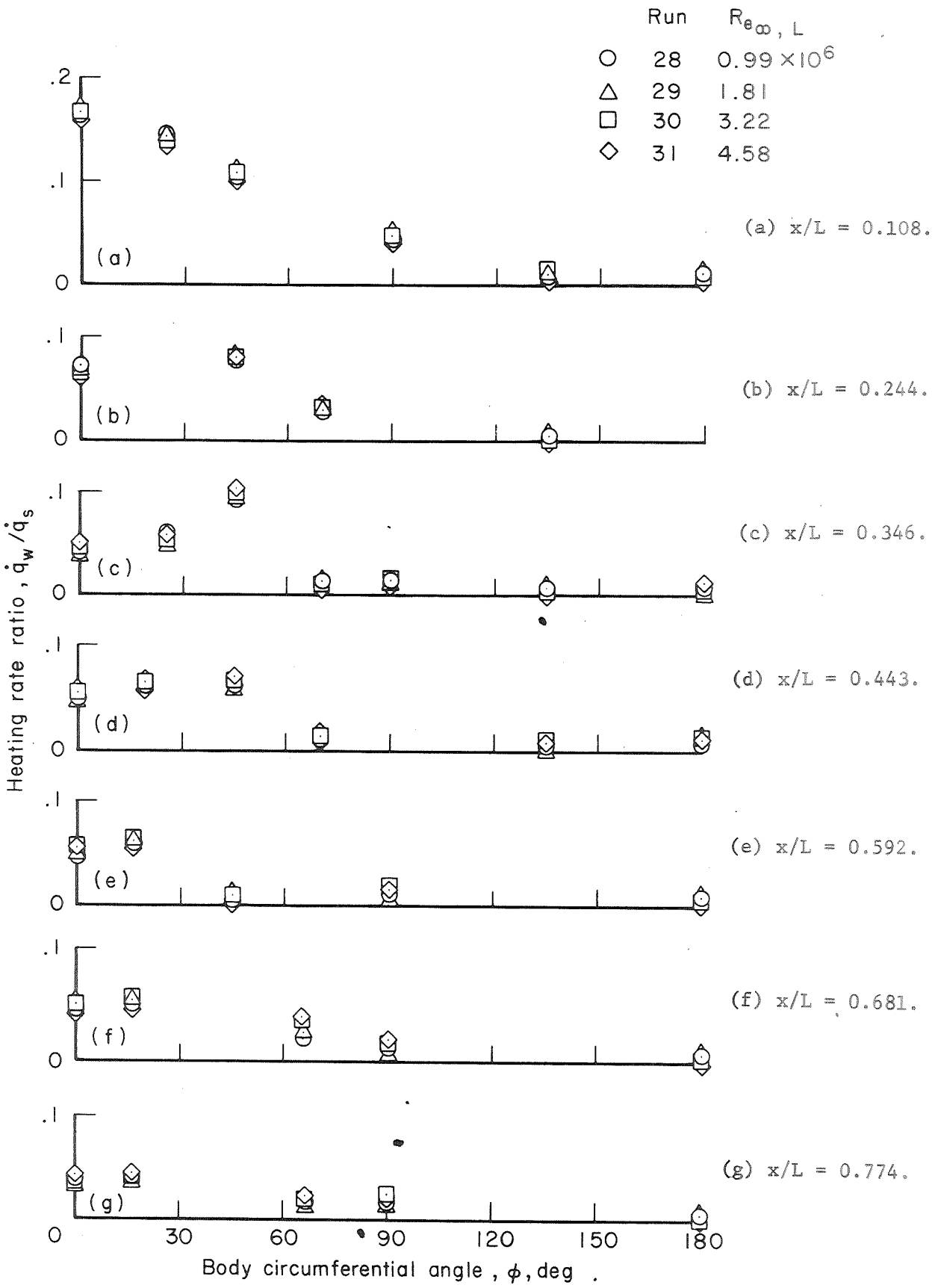

Figure 9.- Body cross-section heating rates; $\alpha = 30°$.

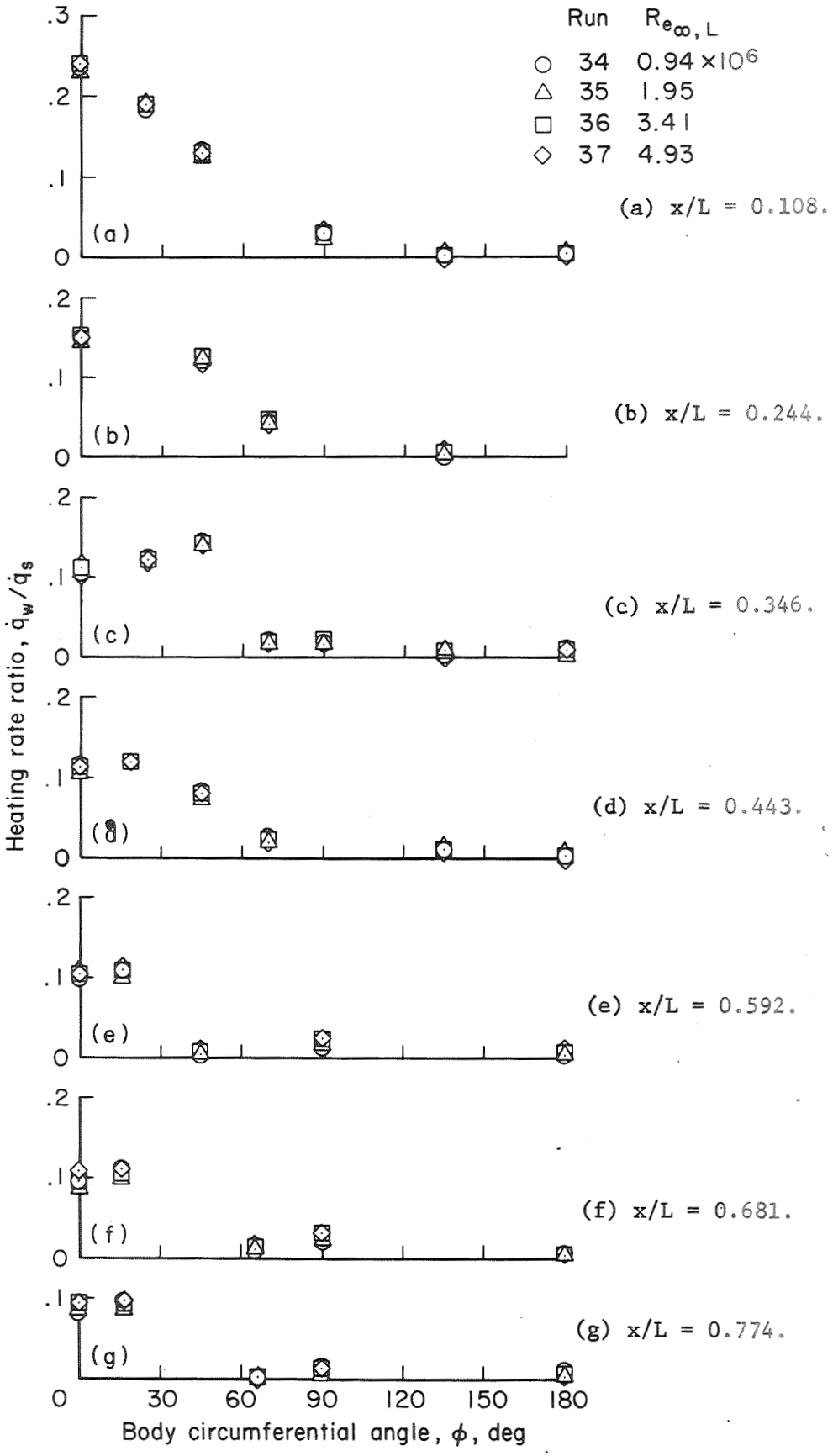

Figure 10.- Body cross-section heating rates; $\alpha = 60°$.

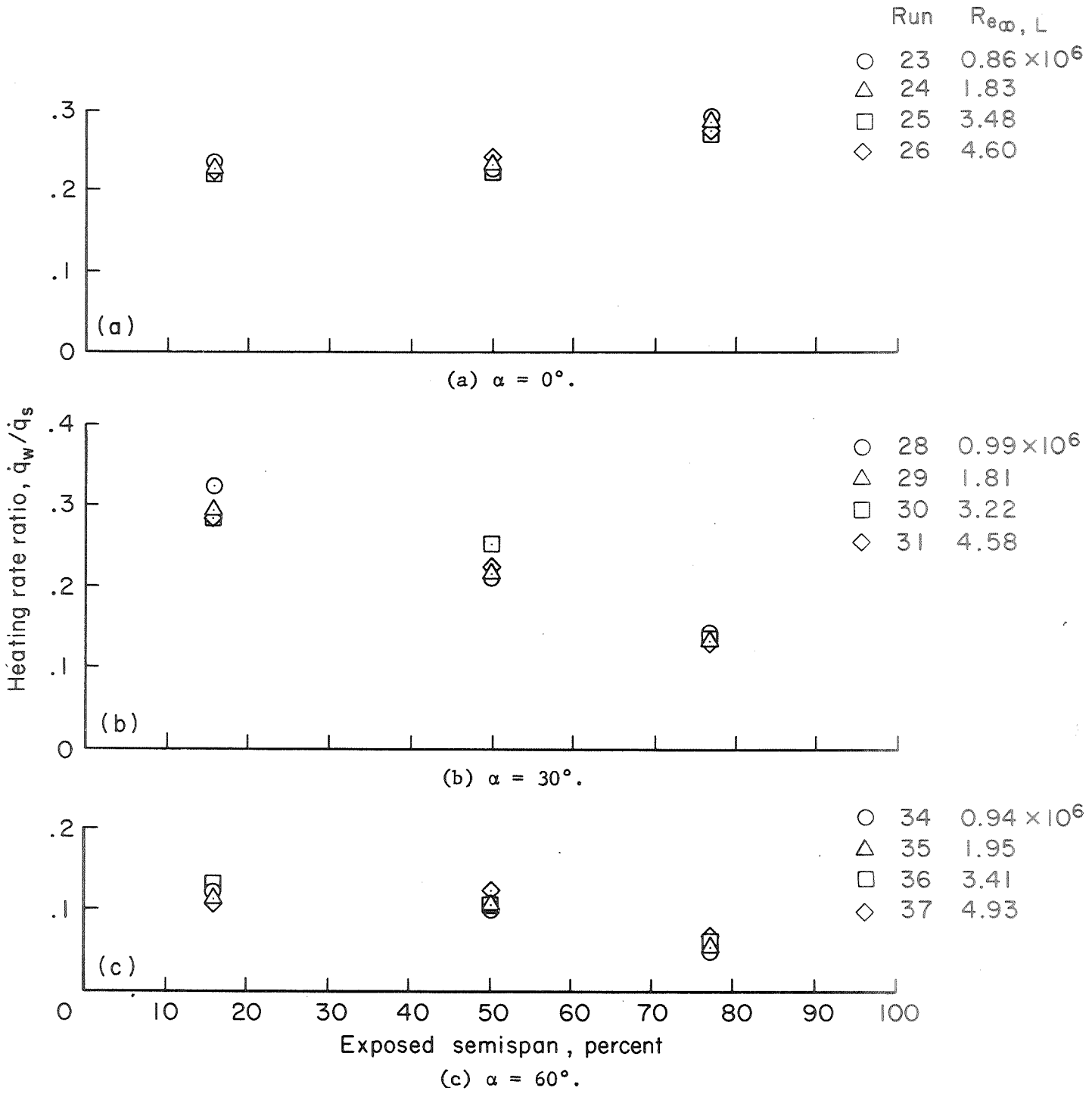

Figure 11.- Spanwise heating rates for wing leading edge.

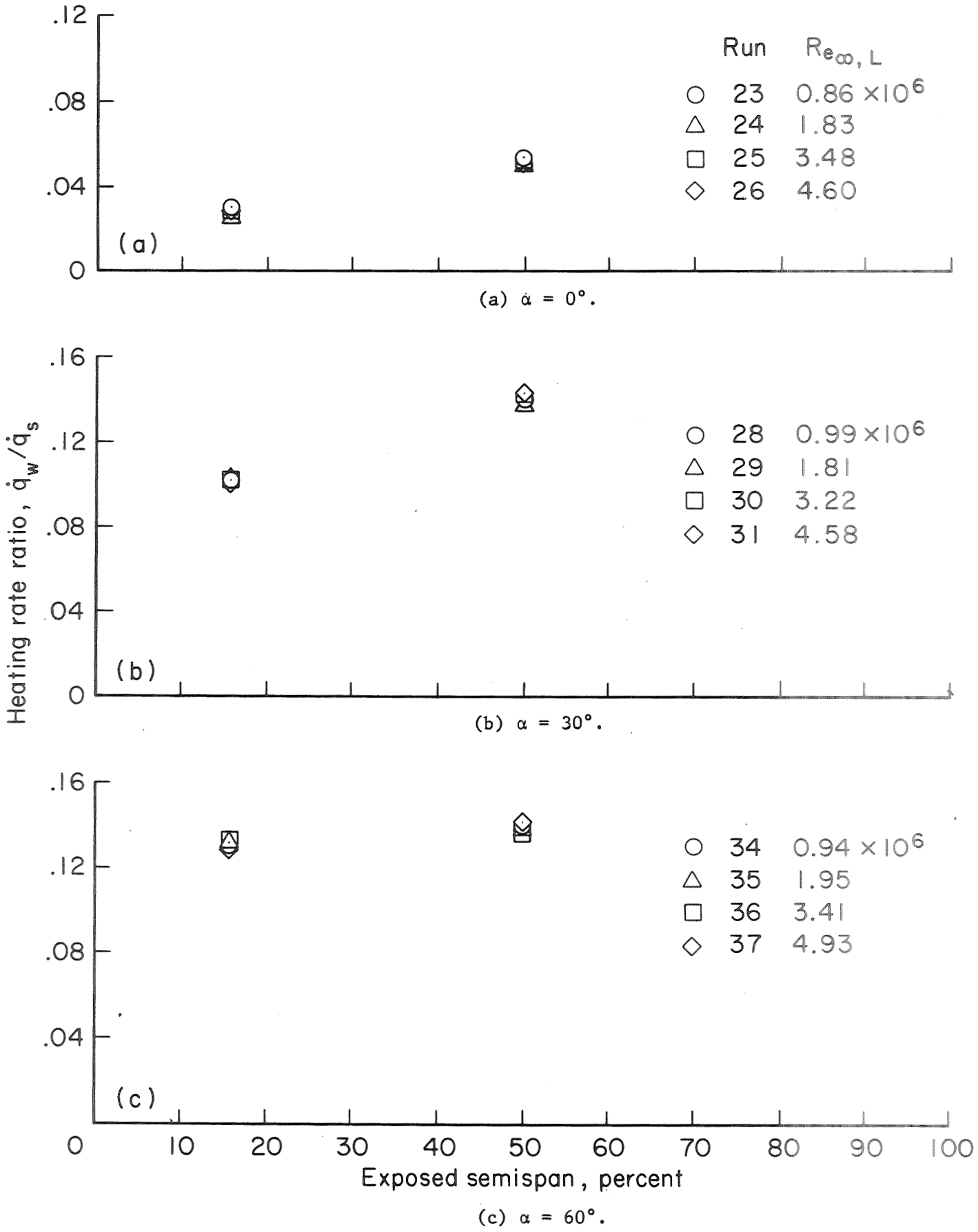

Figure 12.- Spanwise bottom surface heating rates for wing; 10 percent chord.

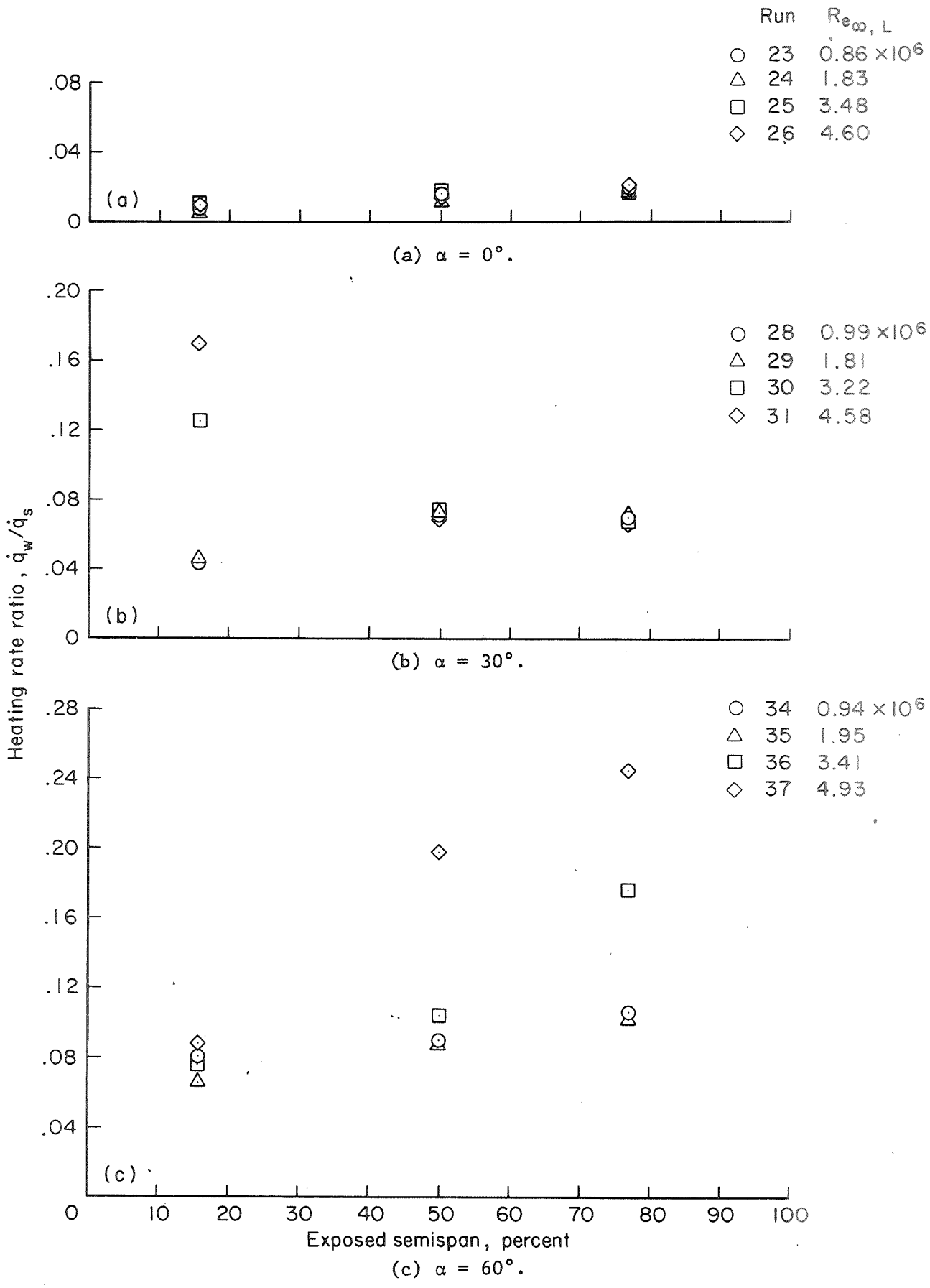

Figure 13.- Spanwise bottom surface heating rates for wing; 50 percent chord.

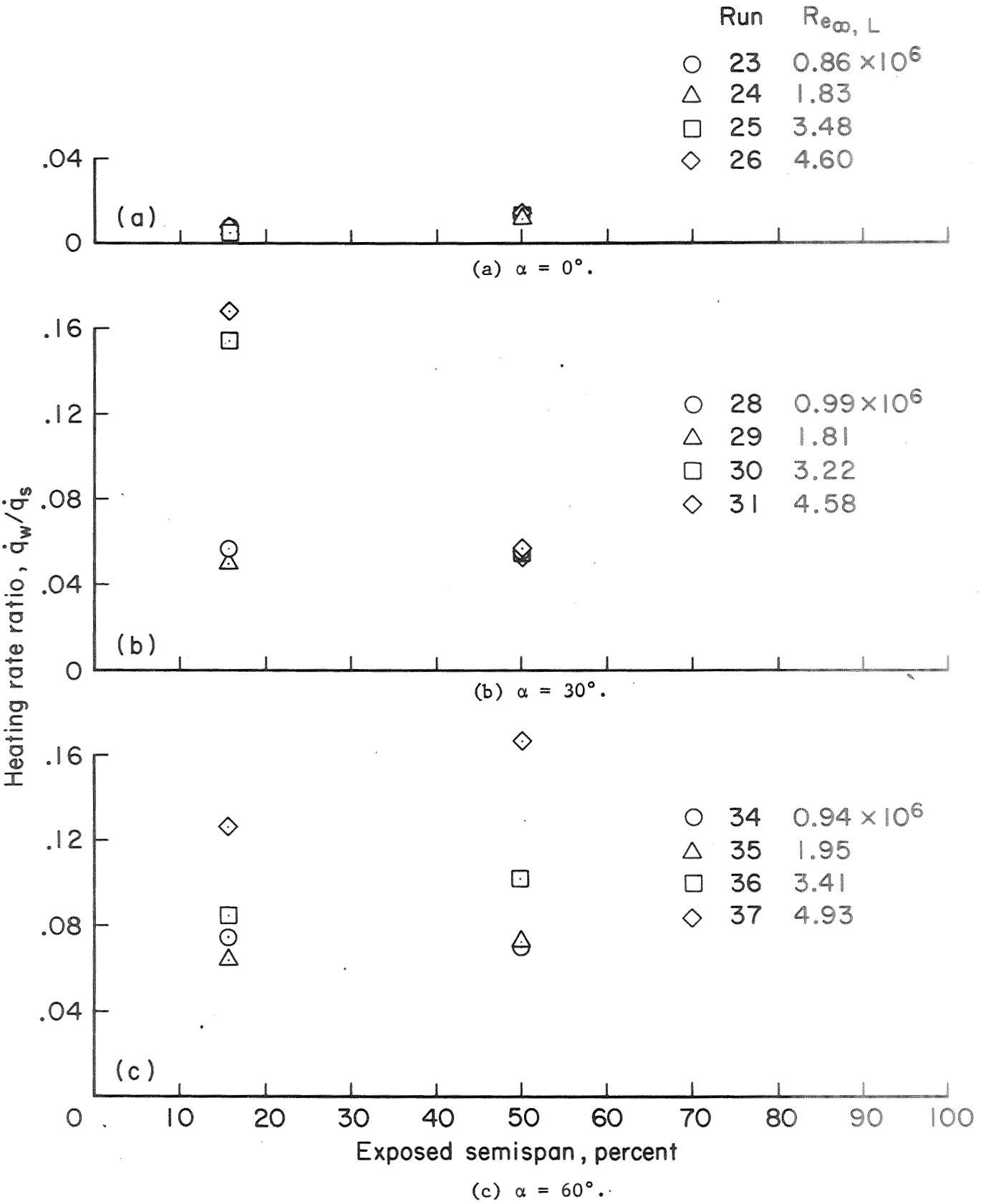

(a) $\alpha = 0°$.

(b) $\alpha = 30°$.

(c) $\alpha = 60°$.

Figure 14.- Spanwise bottom surface heating rates for wing; 75 percent chord.

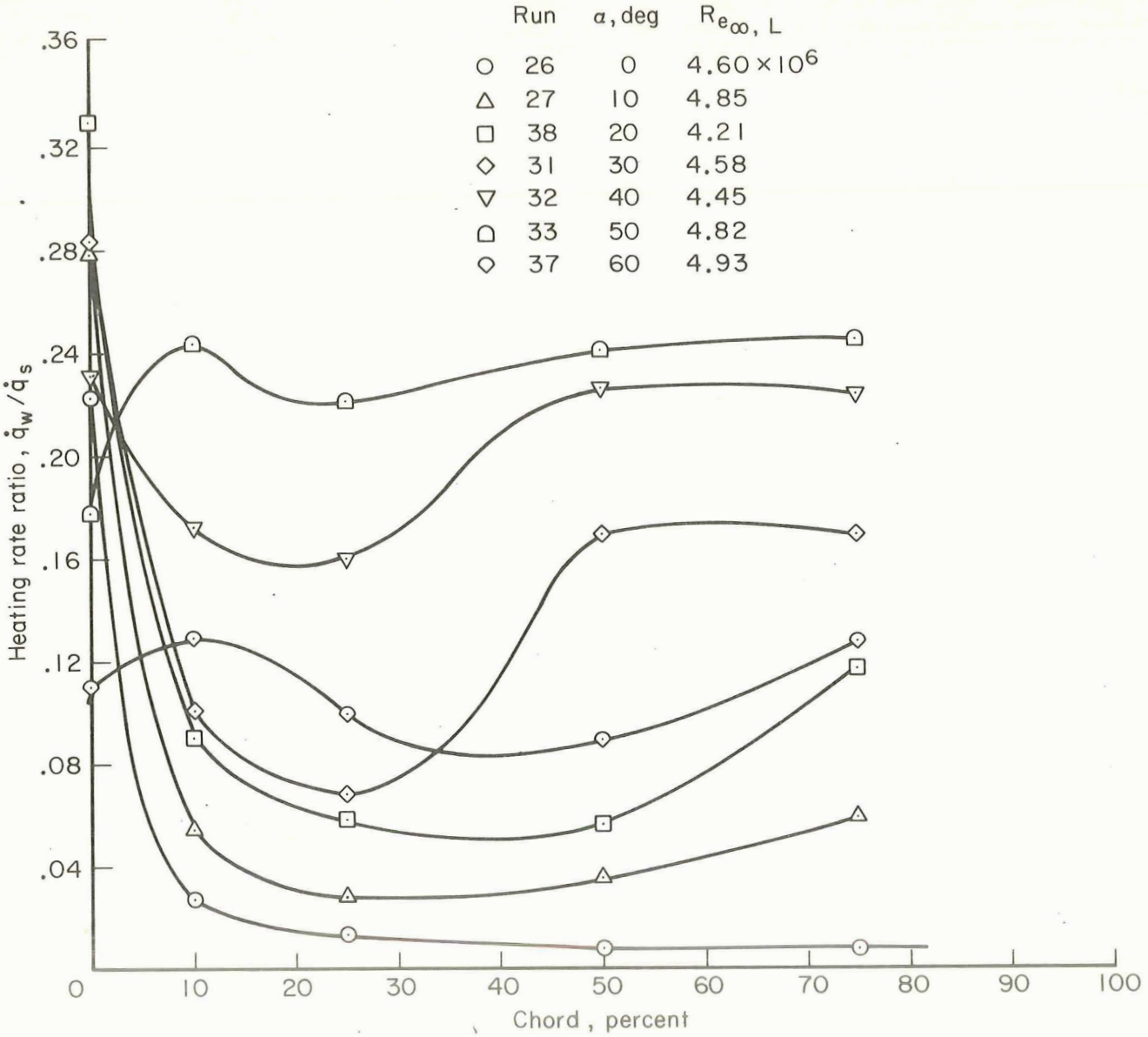

(a) 15.7 percent exposed semispan.

Figure 15.- Effect of angle of attack on chordwise bottom surface heating rates for wing; $Re_{\infty,L} \approx 5 \times 10^6$.

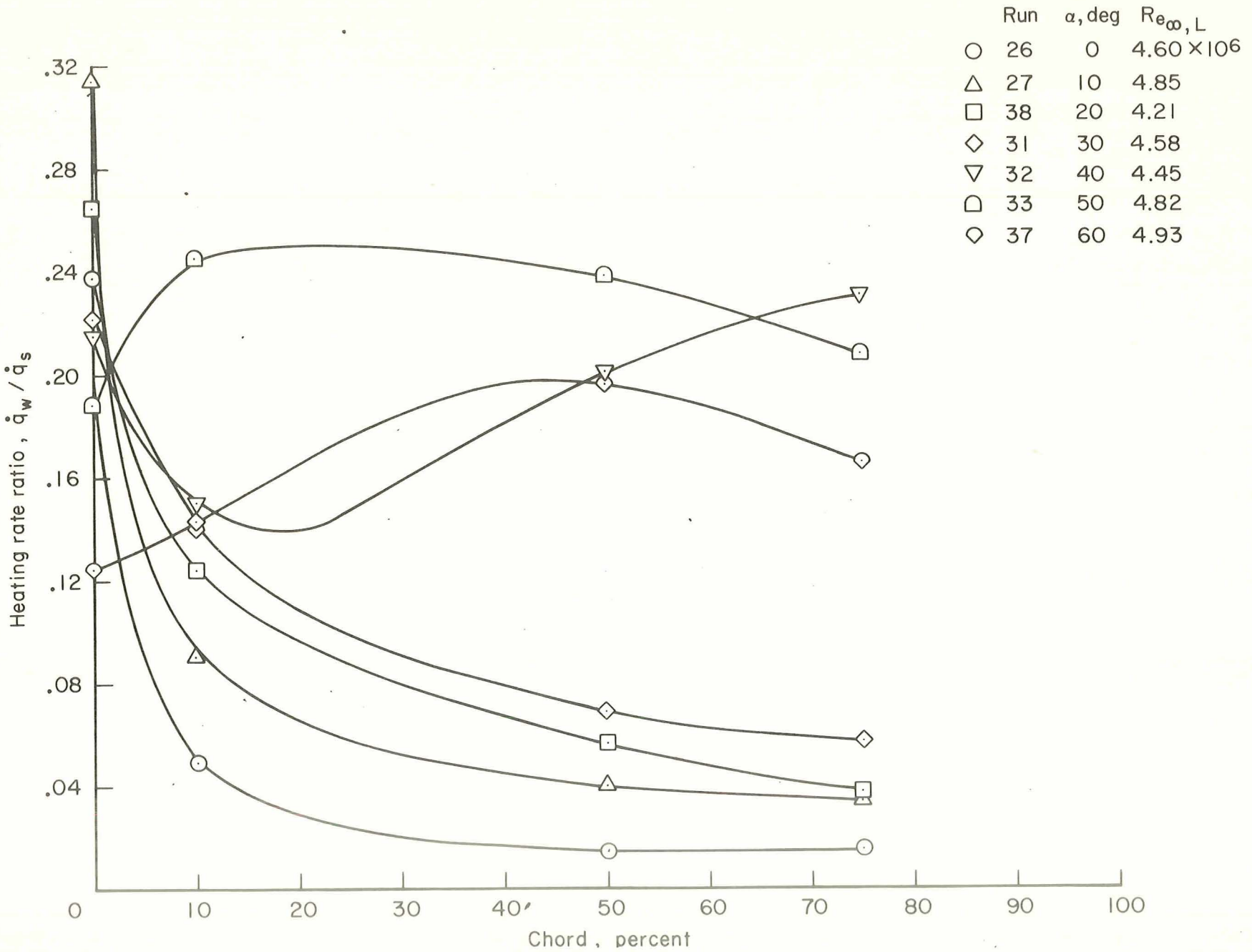

(b) 50 percent exposed semispan.

Figure 15.- Concluded.

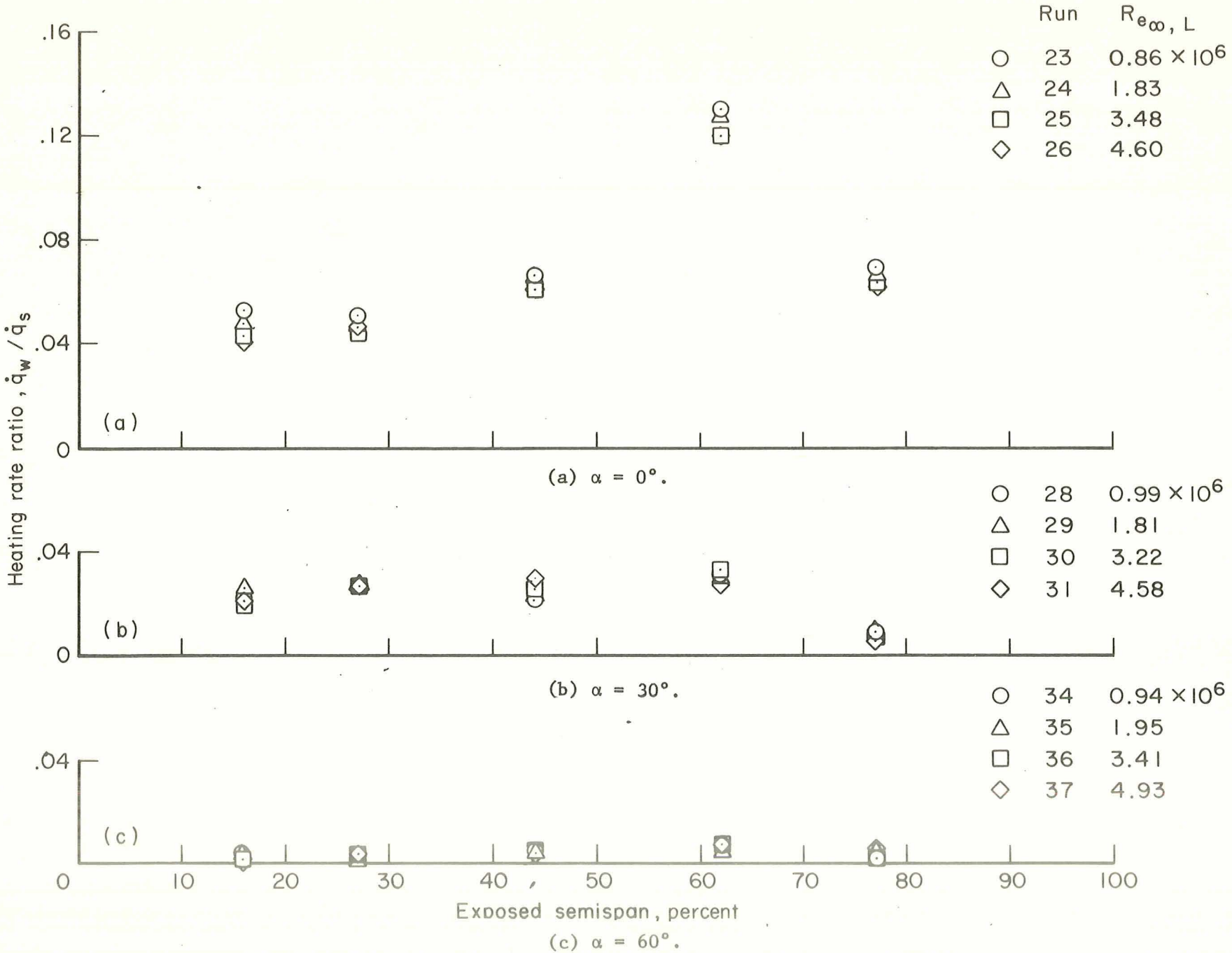

(a) $\alpha = 0°$.

(b) $\alpha = 30°$.

(c) $\alpha = 60°$.

Figure 16.- Spanwise top surface heating rates for wing; 10 percent chord.

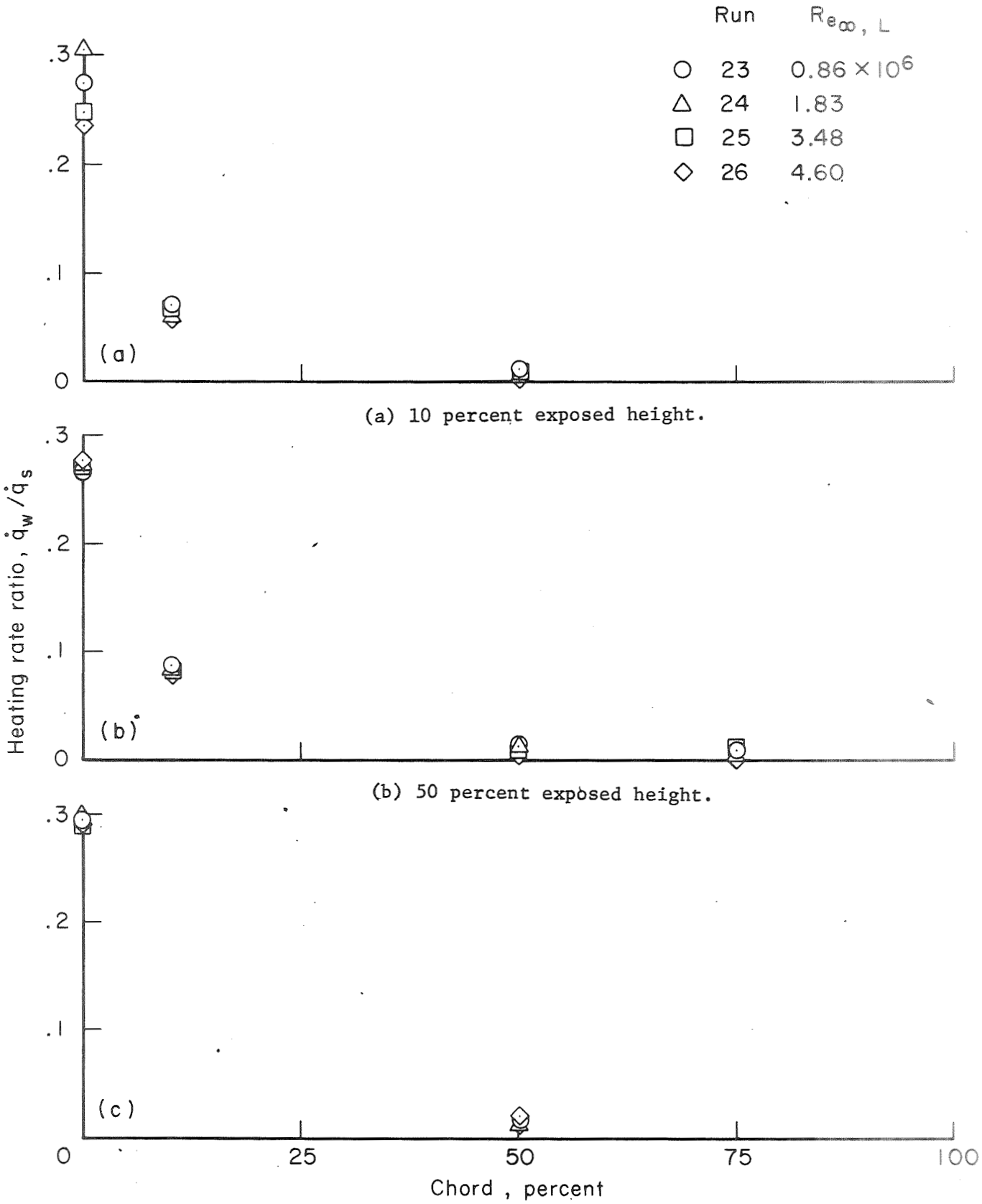

(a) 10 percent exposed height.

(b) 50 percent exposed height.

(c) 75 percent exposed height.

Figure 17.- Chordwise heating rates for vertical tail; $\alpha = 0°$.

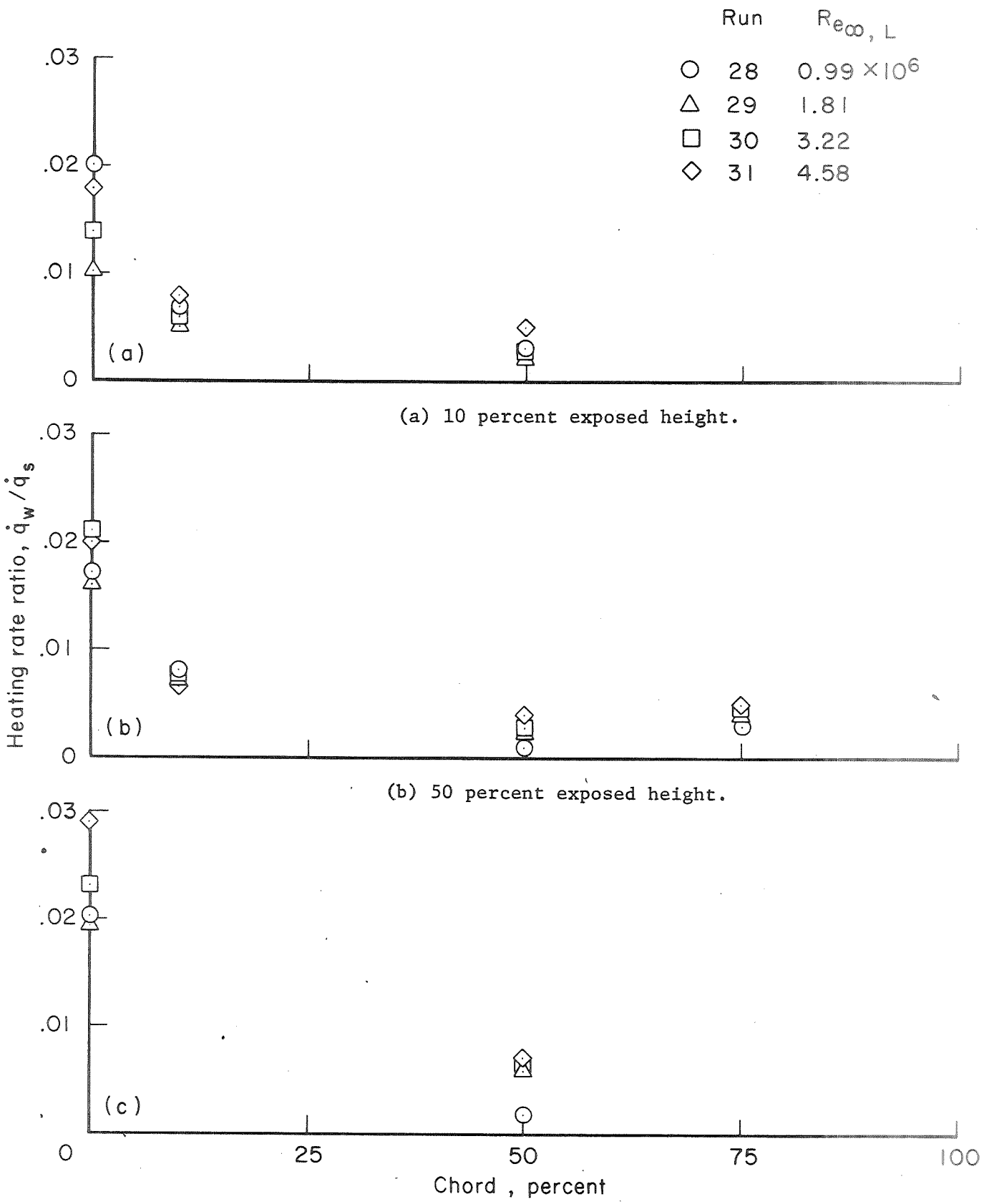

(a) 10 percent exposed height.

(b) 50 percent exposed height.

(c) 75 percent exposed height.

Figure 18.- Chordwise heating rates for vertical tail; $\alpha = 30°$.

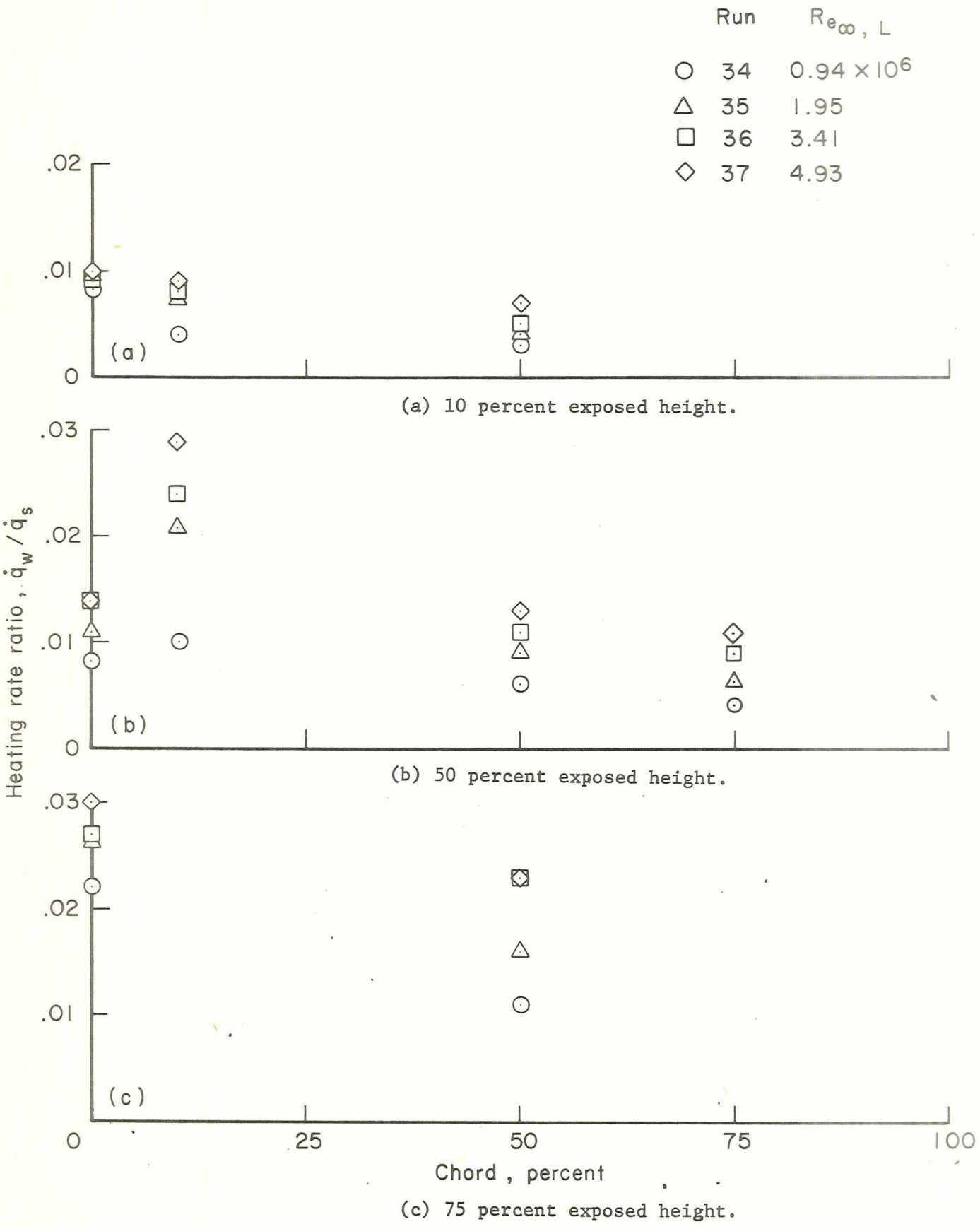

(a) 10 percent exposed height.

(b) 50 percent exposed height.

(c) 75 percent exposed height.

Figure 19.- Chordwise heating rates for vertical tail; $\alpha = 60°$.

TABLE I

THERMOCOUPLE LOCATIONS

DELTA-WING BOOSTER

(a) BODY

T/C No.	X/L	ϕ, deg	T/C No.	X/L	ϕ, deg
1	.027	0	33	.346	135
2	↓	180	34	↓	180
3	.054	0	35	.443	0
4		45	36		19
5		90	37		45
6		135	38		70
7	↓	180	39		90
8	.065	180	40		135
9	.076	159	41	↓	180
10	↓	180	42	.592	0
11	.108	0	43		16
12		25	44		45
13		45	45		70
14		90	46		90
15		135	47		135
16	↓	180	48	↓	180
17	.244	0	49	.681	0
18		25	50		16
19		45	51		65
20		70	52		90
21		90	53		135
22		135	54	↓	180
23	↓	180	55	.774	0
24	.290	0	56		16
25		25	57		66
26		90	58		90
27	↓	180	59		135
28	.346	0	60	↓	180
29		25	61	.867	0
30		45	62		16
31		70	63	↓	90
32	↓	90			

TABLE I.- Concluded

THERMOCOUPLE LOCATIONS

DELTA-WING BOOSTER

(b) WING

T/C No.	% Exposed Semispan	% Chord	Wing Designation
64	15.7	0	left, leading edge
65	↓	10	left, top
66	↓	25	↓
67	↓	50	↓
68	↓	75	↓
69	↓	10	left, bottom
70	↓	25	↓
71	↓	50	↓
72	↓	75	↓
73	26.8	10	left, top
74	38	10	↓
75	↓	25	↓
76	↓	50	↓
77	44	10	↓
78	50	0	left, leading edge
79	↓	10	left, top
80	↓	25	↓
81	↓	50	↓
82	↓	75	↓
83	↓	10	left, bottom
84	↓	50	↓
85	↓	75	↓
86	62	10	left, top
87	↓	50	↓
88	77	0	left, leading edge
89	↓	10	left, top
90	↓	50	↓
91	↓	50	left, bottom

(c) VERTICAL TAIL

T/C No.	% Exposed Height	% Chord	Tail Designation
92	10	0	leading edge
93	↓	10	left side
94	↓	50	↓
95	50	0	leading edge
96	↓	10	left side
97	↓	50	↓
98	↓	75	↓
99	75	0	leading edge
100	↓	50	left side

TABLE II

THERMOCOUPLE CONNECTION SCHEDULE

DELTA-WING BOOSTER

(Test 105 Runs 21-38)

Channel No.	T/C No.	Location	Channel No.	T/C No.	Location
1	1	body	41	54	body
2	2	↓	42	55	↓
3	4		43	56	
4	5		44	57	
5	6		45	58	
6	8		46	60	
7	9		47	61	
8	11		48	62	
9	12		49	63	
10	13		50	64	wing
11	14		51	65	↓
12	15		52	66	
13	16		53	67	
14	17		54	68	
15	19		55	69	
16	20		56	70	
17	22		57	71	
18	24		58	72	
19	28		59	73	
20	29		60	77	
21	30		61	78	
22	31		62	81	
23	32		63	82	
24	33		64	83	
25	34		65	84	
26	35		66	85	
27	36		67	86	
28	37		68	88	
29	38		69	89	
30	40		70	87*	
31	41		71	91	↓
32	42		72	92	tail
33	43		73	93	↓
34	44		74	94	
35	46		75	95	
36	48		76	96	
37	49		77	97	
38	50		78	98	
39	51		79	99	
40	52	↓	80	100	↓

*Note this T/C No. is out of sequence

TABLE III

RUN SCHEDULE

DELTA-WING BOOSTER

(Test 105 Runs 21-38)

M = 7.4

Run	α, deg	$Re_{\infty,L}$
21	-5	0.90×10^6
22	↓	4.88
23	0	.86
24	↓	1.83
25	↓	3.48
26	↓	4.60
27	10	4.85
38	20	4.21
28	30	.99
29	↓	1.81
30	↓	3.22
31	↓	4.58
32	40	4.45
33	50	4.82
34	60	.94
35	↓	1.95
36	↓	3.41
37	↓	4.93

L = 0.410 meter (16.128 in.)
0.006 model scale

APPENDIX A

GD/C B-9J DELTA-WING BOOSTER

DIMENSIONAL DATA

TABLE A-I.- BODY FOR DELTA-WING BOOSTER

MODEL COMPONENT: BODY - B_7

GENERAL DESCRIPTION: BASIC FUSELAGE FOR DELTA WING BOOSTER CONFIGURATION

DRAWING NUMBER: WT-70-105204

DIMENSIONS:	FULL-SCALE	(0.006) MODEL SCALE
Length	219 ft	15.77 in
Max. Width	35 ft	2.52 in
Max. Depth		
Fineness Ratio		
Area		
Max. Cross-Sectional		
Planform	6576 ft^2	34.1 in^2
Wetted		
Base	951.8 ft^2	4.94 in^2

TABLE A-II.- WING FOR DELTA-WING BOOSTER

MODEL COMPONENT: WING - W_5

GENERAL DESCRIPTION: BASIC WING FOR DELTA WING BOOSTER CONFIGURATION

DRAWING NUMBER: WT-70-105204

DIMENSIONS:	FULL-SCALE	0.006 MODEL SCALE
TOTAL DATA		
Area		
Planform	8615 ft^2	44.6 in^2
Wetted		
Span (equivalent)	138.0 ft	9.94 in
Aspect Ratio		
Rate of Taper		
Taper Ratio	0.165	0.165
Diehedral Angle, degrees	5.5	5.5
Incidence Angle, degrees	3.0	3.0
Aerodynamic Twist, degrees	0	0
Toe-In Angle		
Cant Angle		
Sweep Back Angles, degrees		
Leading Edge	53.0	53.0
Trailing Edge	0	0
0.25 Element Line		
Chords:		
Root (Wing Sta. 0.0)	109 ft	7.85 in
Tip, (equivalent)	16.43 ft	1.18 in
MAC	74.36 ft	5.35 in
Fus. Sta. of .25 MAC	53.24 ft	3.83 in
W.P. of .25 MAC		
B.L. of .25 MAC	25.81 ft	1.86 in
Airfoil Section		
Root	NACA 4408	
Tip	NACA 4408	
EXPOSED DATA		
Area	5443 ft^2	28.2 in^2
Span, (equivalent)	106 ft	7.63 ft
Aspect Ratio	2.050	2.050
Taper Ratio	.189	.189
Chords		
Root	87.0 ft	6.26 in
Tip	16.43 ft	1.18 in
MAC	59.74 ft	4.30 in
Fus. Sta. of .25 MAC		
W.P. of .25 MAC	36.71 ft	2.64 in
B.L. of .25 MAC		

TABLE A-III.- VERTICAL TAIL FOR DELTA-WING BOOSTER

MODEL COMPONENT: TAIL - V_3

GENERAL DESCRIPTION: BASIC TAIL FOR DELTA WING BOOSTER CONFIGURATION - VERTICAL TAIL

DRAWING NUMBER: WT-70-105204

DIMENSIONS:	FULL-SCALE	0.006 MODEL SCALE
TOTAL DATA		
Area		
Planform		
Wetted		
Span (equivalent)		
Aspect Ratio		
Rate of Taper		
Taper Ratio		
Dihedral Angle, degrees		
Incidence Angle, degrees		
Aerodynamic Twist, degrees		
Toe-In Angle		
Cant Angle		
Sweep Back Angles, degrees		
Leading Edge		
Trailing Edge		
0.25 Element Line		
Chords:		
Root (Wing Sta. 0.0)		
Tip, (equivalent)		
MAC		
Fus. Sta. of .25 MAC		
W.P. of .25 MAC		
B.L. of .25 MAC		
Airfoil Section		
Root	NACA 0016	
Tip	NACA 0014	
EXPOSED DATA		
Area	1108 ft^2	0.05 in^2
Span, (equivalent)	42.29 ft	3.04 in
Aspect Ratio	1.531	1.531
Taper Ratio	.560	.560
Chords		
Root	35.40 ft	2.55 in
Tip	19.81 ft	1.42 in
MAC	28.24 ft	2.03 in
Fus. Sta. of .25 MAC		
W.P. of .25 MAC		
B.L. of .25 MAC		

APPENDIX B

TABULATED HEAT TRANSFER DATA

GD/C B-9J DELTA-WING BOOSTER
NASA-Ames 3.5-ft HWT
Test 105 Runs 21 - 38

NOMENCLATURE FOR APPENDIX B

CHANNEL	recording-system channel
MACH	free-stream Mach number
PT	free-stream total pressure, psia
QS	stagnation-point heat transfer rate for reference sphere, $Btu/ft^2/sec$
QW	heat transfer rate at model wall for given T/C location, $Btu/ft^2/sec$
QW/QS	heating-rate ratio
REL	free-stream Reynolds number based on model reference length
REYN/FT	free-stream Reynolds number per foot
RSPH	reference sphere radius of one foot at the model scale (i.e., 0.006-ft-radius for these tests), ft
T/C	thermocouple number
TT	free-stream total temperature, °R
TWSPH	reference sphere wall temperature, °R

$\alpha = -5^{\circ}$ TEST NO. 105 RUN NO. 21

MACH	REYN/FT	REL	QS	TWSPH	PT	TT	RSPH(FT)
7.40	6.67E 05	9.00E 05	37.79	561.	154.	1454.	0.006

CHANNEL	T/C	TEMP	QW/QS	CHANNEL	T/C	TEMP	QW/QS
1	1	558.	0.094	41	54	550.	0.008
2	2	563.	0.074	42	55	550.	0.004
3	4	556.	0.054	43	56	550.	0.003
4	5	557.	0.074	44	57	552.	0.019
5	6	558.	0.088	45	58	550.	0.008
6	8	568.	0.368	46	60	551.	0.017
7	9	558.	0.049	47	61	550.	0.007
8	11	553.	0.026	48	62	550.	0.005
9	12	553.	0.027	49	63	550.	0.002
10	13	554.	0.028	50	64	589.	0.210
11	14	554.	0.037	51	65	558.	0.056
12	15	555.	0.067	52	66	553.	0.021
13	16	553.	0.018	53	67	552.	0.015
14	17	551.	0.005	54	68	550.	0.004
15	19	552.	0.011	55	69	554.	0.020
16	20	552.	0.010	56	70	551.	0.009
17	22	552.	0.015	57	71	551.	0.005
18	24	551.	0.003	58	72	551.	0.003
19	28	551.	0.004	59	73	561.	0.063
20	29	551.	0.003	60	77	564.	0.080
21	30	552.	0.011	61	78	587.	0.201
22	31	551.	0.005	62	81	554.	0.013
23	32	551.	0.006	63	82	551.	0.007
24	33	552.	0.012	64	83	556.	0.039
25	34	552.	0.018	65	84	552.	0.010
26	35	551.	0.004	66	85	551.	0.007
27	36	551.	0.003	67	86	571.	0.135
28	37	552.	0.012	68	88	584.	0.276
29	38	551.	0.004	69	89	562.	0.080
30	40	552.	0.012	70	87	552.	0.015
31	41	552.	0.018	71	91	552.	0.009
32	42	551.	0.004	72	92	584.	0.262
33	43	551.	0.004	73	93	559.	0.059
34	44	550.	0.003	74	94	553.	0.013
35	46	550.	0.006	75	95	586.	0.322
36	48	551.	0.014	76	96	565.	0.101
37	49	550.	0.005	77	97	553.	0.017
38	50	550.	0.003	78	98	553.	0.008
39	51	550.	0.008	79	99	590.	0.368
40	52	550.	0.003	80	100	553.	0.024

$\alpha = -5°$ TEST NO. 105 RUN NO. 22

MACH	REYN/FT	REL	QS	TWSPH	PT	TT	RSPH(FT)
7.40	3.63E 06	4.88E 06	76.48	572.	770.	1384.	0.006

CHANNEL	T/C	TEMP	QW/QS	CHANNEL	T/C	TEMP	QW/QS
1	1	567.	0.089	41	54	554.	0.013
2	2	576.	0.073	42	55	554.	0.006
3	4	563.	0.052	43	56	554.	0.008
4	5	565.	0.072	44	57	557.	0.026
5	6	567.	0.087	45	58	554.	0.011
6	8	596.	0.527	46	60	556.	0.024
7	9	574.	0.073	47	61	553.	0.006
8	11	559.	0.024	48	62	554.	0.008
9	12	559.	0.025	49	63	555.	0.021
10	13	559.	0.027	50	64	610.	0.201
11	14	560.	0.035	51	65	571.	0.057
12	15	568.	0.110	52	66	560.	0.022
13	16	557.	0.015	53	67	555.	0.011
14	17	556.	0.004	54	68	553.	0.003
15	19	557.	0.009	55	69	559.	0.018
16	20	556.	0.008	56	70	555.	0.009
17	22	557.	0.013	57	71	554.	0.004
18	24	556.	0.003	58	72	554.	0.002
19	28	555.	0.003	59	73	572.	0.062
20	29	555.	0.002	60	77	577.	0.079
21	30	557.	0.012	61	78	606.	0.210
22	31	555.	0.005	62	81	557.	0.014
23	32	556.	0.006	63	82	555.	0.006
24	33	556.	0.011	64	83	564.	0.035
25	34	559.	0.032	65	84	556.	0.009
26	35	555.	0.006	66	85	555.	0.005
27	36	555.	0.004	67	86	594.	0.137
28	37	556.	0.011	68	88	616.	0.266
29	38	554.	0.005	69	89	575.	0.075
30	40	557.	0.018	70	87	560.	0.017
31	41	559.	0.027	71	91	557.	0.010
32	42	555.	0.010	72	92	614.	0.246
33	43	555.	0.009	73	93	571.	0.061
34	44	554.	0.002	74	94	556.	0.008
35	46	554.	0.007	75	95	619.	0.317
36	48	556.	0.025	76	96	580.	0.103
37	49	554.	0.005	77	97	556.	0.014
38	50	554.	0.009	78	98	554.	0.008
39	51	554.	0.009	79	99	626.	0.372
40	52	553.	0.004	80	100	556.	0.024

$\alpha = 0^{\circ}$ TEST NO. 105 RUN NO. 23

MACH	REYN/FT	REI	OS	TWSPH	PT	TT	RSPH(FT)
7.40	6.38E 05	8.60E 05	39.57	565.	154.	1495.	0.006

CHANNEL	T/C	TEMP	QW/QS	CHANNEL	T/C	TEMP	QW/QS
1	1	562.	0.124	41	54	554.	0.008
2	2	563.	0.062	42	55	554.	0.004
3	4	559.	0.074	43	56	554.	0.006
4	5	559.	0.075	44	57	555.	0.027
5	6	559.	0.076	45	58	554.	0.004
6	8	566.	0.311	46	60	554.	0.009
7	9	558.	0.035	47	61	554.	0.003
8	11	557.	0.044	48	62	554.	0.005
9	12	557.	0.042	49	63	671.	0.002
10	13	557.	0.040	50	64	585.	0.235
11	14	556.	0.039	51	65	561.	0.052
12	15	556.	0.042	52	66	556.	0.017
13	16	555.	0.016	53	67	554.	0.006
14	17	555.	0.009	54	68	553.	0.003
15	19	556.	0.017	55	69	559.	0.030
16	20	555.	0.013	56	70	556.	0.015
17	22	555.	0.009	57	71	555.	0.008
18	24	555.	0.006	58	72	555.	0.007
19	28	554.	0.004	59	73	562.	0.051
20	29	555.	0.006	60	77	565.	0.066
21	30	556.	0.022	61	78	586.	0.224
22	31	554.	0.005	62	81	557.	0.012
23	32	554.	0.006	63	82	554.	0.005
24	33	554.	0.005	64	83	562.	0.053
25	34	554.	0.010	65	84	556.	0.015
26	35	554.	0.006	66	85	555.	0.011
27	36	554.	0.006	67	86	573.	0.130
28	37	556.	0.026	68	88	587.	0.289
29	38	554.	0.006	69	89	563.	0.069
30	40	555.	0.004	70	87	555.	0.012
31	41	555.	0.012	71	91	556.	0.018
32	42	555.	0.007	72	92	576.	0.279
33	43	555.	0.007	73	93	564.	0.069
34	44	554.	0.008	74	94	555.	0.011
35	46	554.	0.005	75	95	583.	0.270
36	48	555.	0.015	76	96	565.	0.086
37	49	554.	0.004	77	97	555.	0.013
38	50	554.	0.005	78	98	553.	0.008
39	51	554.	0.006	79	99	585.	0.292
40	52	564.	0.003	80	100	555.	0.017

$\alpha = 0^{\circ}$ TEST NO. 105 RUN NO. 24

MACH	REYN/FT	REL	OS	TWSPH	PT	TT	RSPH(FT)
7.40	1.36E 06	1.83E 06	56.08	562.	322.	1477.	0.006

CHANNEL	T/C	TEMP	QW/QS	CHANNEL	T/C	TEMP	QW/QS
1	1	558.	0.121	41	54	550.	0.006
2	2	558.	0.059	42	55	551.	0.004
3	4	554.	0.071	43	56	550.	0.003
4	5	554.	0.072	44	57	553.	0.028
5	6	554.	0.073	45	58	550.	0.005
6	8	563.	0.365	46	60	551.	0.008
7	9	554.	0.040	47	61	551.	0.003
8	11	551.	0.043	48	62	550.	0.005
9	12	551.	0.040	49	63	673.	0.002
10	13	550.	0.038	50	64	587.	0.227
11	14	550.	0.037	51	65	560.	0.048
12	15	551.	0.054	52	66	553.	0.016
13	16	549.	0.013	53	67	552.	0.006
14	17	548.	0.010	54	68	551.	0.002
15	19	549.	0.017	55	69	556.	0.027
16	20	548.	0.012	56	70	553.	0.013
17	22	548.	0.012	57	71	553.	0.009
18	24	548.	0.004	58	72	553.	0.007
19	28	548.	0.004	59	73	561.	0.048
20	29	548.	0.005	60	77	565.	0.065
21	30	550.	0.022	61	78	590.	0.231
22	31	548.	0.005	62	81	555.	0.011
23	32	548.	0.005	63	82	552.	0.005
24	33	548.	0.005	64	83	561.	0.050
25	34	548.	0.011	65	84	554.	0.014
26	35	548.	0.005	66	85	553.	0.011
27	36	548.	0.005	67	86	574.	0.128
28	37	550.	0.026	68	88	592.	0.235
29	38	548.	0.005	69	89	563.	0.065
30	40	551.	0.004	70	87	552.	0.012
31	41	551.	0.014	71	91	555.	0.016
32	42	551.	0.005	72	92	580.	0.302
33	43	551.	0.007	73	93	561.	0.062
34	44	550.	0.006	74	94	550.	0.010
35	46	550.	0.004	75	95	583.	0.270
36	48	551.	0.013	76	96	563.	0.081
37	49	550.	0.003	77	97	550.	0.011
38	50	550.	0.004	78	98	548.	0.007
39	51	550.	0.006	79	99	586.	0.295
40	52	551.	0.002	80	100	550.	0.016

$\alpha = 0^{\circ}$

TEST NO. 105 RUN NO. 25

MACH	REYN/FT	REL	QS	TWSPH	PT	TT	RSPH(FT)
7.40	2.58E 06	3.48E 06	63.24	559.	537.	1366.	0.006

CHANNEL	T/C	TEMP	QW/QS	CHANNEL	T/C	TEMP	QW/QS
1	1	554.	0.119	41	54	547.	0.007
2	2	555.	0.058	42	55	549.	0.004
3	4	549.	0.072	43	56	548.	0.003
4	5	549.	0.069	44	57	551.	0.030
5	6	549.	0.071	45	58	548.	0.007
6	8	564.	0.404	46	60	548.	0.011
7	9	551.	0.046	47	61	549.	0.003
8	11	547.	0.041	48	62	549.	0.003
9	12	546.	0.038	49	63	664.	0.0
10	13	546.	0.037	50	64	592.	0.217
11	14	545.	0.035	51	65	558.	0.042
12	15	547.	0.063	52	66	552.	0.014
13	16	544.	0.012	53	67	550.	0.005
14	17	544.	0.008	54	68	549.	0.001
15	19	545.	0.016	55	69	555.	0.026
16	20	544.	0.011	56	70	551.	0.013
17	22	544.	0.012	57	71	551.	0.006
18	24	544.	0.004	58	72	551.	0.005
19	28	544.	0.003	59	73	560.	0.045
20	29	544.	0.005	60	77	564.	0.062
21	30	547.	0.023	61	78	595.	0.219
22	31	544.	0.005	62	81	550.	0.008
23	32	544.	0.004	63	82	550.	0.004
24	33	544.	0.004	64	83	561.	0.049
25	34	545.	0.013	65	84	553.	0.013
26	35	545.	0.005	66	85	552.	0.011
27	36	545.	0.006	67	86	575.	0.120
28	37	547.	0.028	68	88	600.	0.266
29	38	544.	0.005	69	89	564.	0.063
30	40	547.	0.005	70	87	551.	0.010
31	41	547.	0.016	71	91	554.	0.015
32	42	548.	0.003	72	92	590.	0.247
33	43	548.	0.006	73	93	560.	0.062
34	44	547.	0.004	74	94	548.	0.009
35	46	547.	0.003	75	95	589.	0.273
36	48	548.	0.015	76	96	564.	0.079
37	49	548.	0.002	77	97	548.	0.013
38	50	548.	0.005	78	98	546.	0.007
39	51	548.	0.006	79	99	593.	0.290
40	52	560.	0.002	80	100	549.	0.017

$\alpha = 0^{\circ}$

TEST NO. 105 RUN NO. 26

MACH	REYN/FT	REL	QS	TWSPH	PT	TT	RSPH(FT)
7.40	3.42E 06	4.60E 06	30.78	564.	762.	1424.	0.006

CHANNEL	T/C	TEMP	QW/QS	CHANNEL	T/C	TEMP	QW/QS
1	1	558.	0.118	41	54	548.	0.009
2	2	558.	0.058	42	55	550.	0.004
3	4	552.	0.073	43	56	549.	0.003
4	5	552.	0.069	44	57	553.	0.030
5	6	552.	0.072	45	58	549.	0.007
6	8	588.	0.403	46	60	550.	0.015
7	9	555.	0.050	47	61	551.	0.003
8	11	549.	0.042	48	62	550.	0.003
9	12	548.	0.038	49	63	550.	0.011
10	13	548.	0.027	50	64	600.	0.222
11	14	547.	0.035	51	65	561.	0.041
12	15	551.	0.072	52	66	554.	0.013
13	16	545.	0.011	53	67	551.	0.006
14	17	545.	0.008	54	68	551.	0.002
15	19	547.	0.017	55	69	557.	0.027
16	20	545.	0.011	56	70	553.	0.013
17	22	545.	0.012	57	71	553.	0.007
18	24	545.	0.004	58	72	553.	0.007
19	28	545.	0.003	59	73	564.	0.046
20	29	545.	0.005	60	77	568.	0.062
21	30	549.	0.023	61	78	604.	0.238
22	31	545.	0.005	62	81	552.	0.010
23	32	545.	0.004	63	82	552.	0.004
24	33	545.	0.004	64	83	565.	0.049
25	34	546.	0.016	65	84	556.	0.014
26	35	546.	0.005	66	85	556.	0.014
27	36	546.	0.005	67	86	581.	0.120
28	37	549.	0.027	68	88	608.	0.270
29	38	546.	0.005	69	89	569.	0.062
30	40	547.	0.007	70	97	553.	0.013
31	41	548.	0.021	71	91	557.	0.020
32	42	548.	0.005	72	92	596.	0.233
33	43	549.	0.007	73	93	564.	0.058
34	44	548.	0.004	74	94	550.	0.009
35	46	547.	0.003	75	95	596.	0.274
36	48	549.	0.019	76	96	568.	0.079
37	49	549.	0.003	77	97	551.	0.012
38	50	549.	0.005	78	98	548.	0.003
39	51	549.	0.008	79	99	601.	0.294
40	52	548.	0.002	80	100	552.	0.018

$\alpha = 10^{\circ}$ TEST NO. 105 RUN NO. 27

MACH	REYN/FT	PEL	OS	TVSPH	PT	TT	RSPH(FT)
7.40	3.61E 06	4.95E 06	74.97	589.	763.	1380.	0.006

CHANNEL	T/C	TEMP	QW/QS	CHANNEL	T/C	TEMP	QW/QS
1	1	570.	0.187	41	54	551.	0.011
2	2	559.	0.031	42	55	554.	0.025
3	4	563.	0.111	43	56	554.	0.026
4	5	559.	0.069	44	57	553.	0.028
5	6	557.	0.045	45	58	551.	0.009
6	8	561.	0.212	46	60	552.	0.023
7	9	555.	0.019	47	61	555.	0.039
8	11	560.	0.083	48	62	556.	0.043
9	12	559.	0.074	49	63	552.	0.018
10	13	558.	0.063	50	64	610.	0.278
11	14	555.	0.039	51	65	558.	0.029
12	15	553.	0.016	52	66	552.	0.005
13	16	553.	0.013	53	67	550.	0.002
14	17	554.	0.021	54	68	551.	0.001
15	19	557.	0.035	55	69	566.	0.054
16	20	553.	0.017	56	70	559.	0.028
17	22	552.	0.004	57	71	562.	0.035
18	24	554.	0.013	58	72	570.	0.058
19	28	553.	0.010	59	73	561.	0.038
20	29	554.	0.017	60	77	565.	0.055
21	30	559.	0.049	61	78	616.	0.313
22	31	552.	0.008	62	81	554.	0.007
23	32	552.	0.007	63	82	552.	0.002
24	33	552.	0.001	64	83	576.	0.091
25	34	553.	0.016	65	84	564.	0.040
26	35	553.	0.011	66	85	564.	0.033
27	36	555.	0.022	67	86	577.	0.111
28	37	555.	0.039	68	88	594.	0.237
29	38	552.	0.008	69	89	562.	0.039
30	40	552.	0.002	70	87	556.	0.008
31	41	553.	0.014	71	91	563.	0.033
32	42	554.	0.014	72	92	569.	0.092
33	43	555.	0.022	73	93	560.	0.038
34	44	551.	0.006	74	94	551.	0.002
35	46	551.	0.007	75	95	573.	0.108
36	48	552.	0.016	76	96	560.	0.035
37	49	553.	0.020	77	97	554.	0.007
38	50	553.	0.019	78	98	552.	0.006
39	51	551.	0.005	79	99	582.	0.187
40	52	551.	0.006	80	100	554.	0.011

$\alpha = 30^{\circ}$

TEST NO. 105 RUN NO. 28

MACH	REYN/FT	REL	OS	TwSPH	PT	TT	RSPH(FT)
7.40	7.37E 05	9.00E 05	30.55	558.	144.	1315.	0.006

CHANNEL	T/C	TEMP	QW/QS	CHANNEL	T/C	TEMP	QW/QS
1	1	552.	0.302	41	54	540.	0.005
2	2	542.	0.000	42	55	543.	0.039
3	4	547.	0.167	43	56	543.	0.040
4	5	543.	0.060	44	57	541.	0.012
5	6	542.	0.019	45	58	541.	0.022
6	8	542.	0.026	46	60	541.	0.005
7	9	542.	0.002	47	61	543.	0.036
8	11	548.	0.158	48	62	543.	0.036
9	12	547.	0.132	49	63	541.	0.013
10	13	545.	0.101	50	64	566.	0.323
11	14	543.	0.036	51	65	543.	0.022
12	15	542.	0.007	52	66	541.	0.005
13	16	542.	0.004	53	67	540.	0.002
14	17	545.	0.068	54	68	540.	0.0
15	19	546.	0.075	55	69	553.	0.102
16	20	543.	0.027	56	70	549.	0.065
17	22	542.	0.002	57	71	547.	0.044
18	24	544.	0.051	58	72	549.	0.056
19	23	544.	0.045	59	73	543.	0.025
20	29	544.	0.054	60	77	543.	0.022
21	30	547.	0.098	61	78	561.	0.210
22	31	541.	0.013	62	81	538.	0.010
23	32	542.	0.011	63	82	539.	0.002
24	33	541.	0.002	64	83	557.	0.138
25	34	542.	0.007	65	84	550.	0.071
26	35	545.	0.051	66	85	547.	0.055
27	36	545.	0.063	67	86	540.	0.030
28	37	544.	0.068	68	88	554.	0.142
29	38	541.	0.013	69	89	540.	0.009
30	40	542.	0.002	70	87	538.	0.010
31	41	542.	0.008	71	91	548.	0.069
32	42	545.	0.051	72	92	543.	0.020
33	43	545.	0.056	73	93	541.	0.007
34	44	541.	0.006	74	94	541.	0.003
35	45	541.	0.011	75	95	543.	0.017
36	48	541.	0.008	76	96	541.	0.009
37	49	543.	0.047	77	97	540.	0.001
38	50	543.	0.049	78	98	540.	0.003
39	51	541.	0.020	79	99	542.	0.020
40	52	541.	0.011	80	100	540.	0.002

$\alpha = 30^{\circ}$ TEST NO. 105 RUN NO. 29

MACH	REYN/FT	REI	OS	TWSPH	PT	TT	RSPH(FT)
7.40	1.34E 06	1.81E 06	55.66	575.	321.	1483.	0.006

CHANNEL	T/C	TEMP	QW/QS	CHANNEL	T/C	TEMP	QW/QS
1	1	564.	0.304	41	54	545.	0.003
2	2	545.	0.008	42	55	551.	0.037
3	4	556.	0.170	43	56	551.	0.041
4	5	548.	0.062	44	57	546.	0.013
5	6	545.	0.020	45	58	547.	0.023
6	8	547.	0.041	46	60	545.	0.003
7	9	544.	0.003	47	61	551.	0.031
8	11	556.	0.161	48	62	551.	0.040
9	12	554.	0.135	49	63	546.	0.017
10	13	552.	0.104	50	64	594.	0.292
11	14	547.	0.038	51	65	549.	0.020
12	15	545.	0.008	52	66	546.	0.005
13	16	545.	0.004	53	67	544.	0.001
14	17	552.	0.069	54	68	544.	0.000
15	19	553.	0.075	55	69	569.	0.101
16	20	547.	0.027	56	70	562.	0.065
17	22	545.	0.002	57	71	561.	0.045
18	24	551.	0.054	58	72	562.	0.049
19	28	551.	0.047	59	73	550.	0.027
20	29	552.	0.058	60	77	548.	0.023
21	30	556.	0.098	61	78	587.	0.216
22	31	546.	0.012	62	81	542.	0.010
23	32	546.	0.011	63	82	543.	0.002
24	33	545.	0.001	64	83	577.	0.137
25	34	546.	0.009	65	84	564.	0.072
26	35	553.	0.049	66	85	560.	0.051
27	36	554.	0.065	67	86	549.	0.030
28	37	551.	0.067	68	88	571.	0.138
29	38	546.	0.013	69	89	544.	0.009
30	40	546.	0.002	70	87	545.	0.008
31	41	547.	0.012	71	91	563.	0.068
32	42	554.	0.052	72	92	549.	0.010
33	43	555.	0.057	73	93	547.	0.005
34	44	545.	0.006	74	94	546.	0.002
35	46	546.	0.012	75	95	549.	0.016
36	48	545.	0.008	76	96	546.	0.007
37	49	551.	0.050	77	97	545.	0.002
38	50	551.	0.053	78	98	545.	0.004
39	51	547.	0.026	79	99	547.	0.019
40	52	546.	0.012	80	100	545.	0.006

$\alpha = 30^{\circ}$ TEST NO. 105 RUN NO. 30

MACH	REYN/FT	REI	QS	TWSPH	PT	TT	RSPH(FT)
7.40	2.40E 06	3.22E 06	68.31	582.	545.	1440.	0.006

CHANNEL	T/C	TEMP	QW/QS	CHANNEL	T/C	TEMP	QW/QS
1	1	568.	0.305	41	54	544.	0.003
2	2	543.	0.008	42	55	553.	0.038
3	4	557.	0.172	43	56	553.	0.042
4	5	546.	0.062	44	57	546.	0.016
5	6	543.	0.019	45	58	546.	0.023
6	8	547.	0.053	46	60	544.	0.003
7	9	541.	0.003	47	61	554.	0.033
8	11	557.	0.163	48	62	554.	0.039
9	12	554.	0.137	49	63	546.	0.018
10	13	551.	0.105	50	64	608.	0.283
11	14	544.	0.038	51	65	550.	0.021
12	15	542.	0.007	52	66	545.	0.005
13	16	542.	0.005	53	67	544.	0.001
14	17	551.	0.069	54	68	544.	0.000
15	19	553.	0.076	55	69	578.	0.101
16	20	544.	0.028	56	70	570.	0.066
17	22	542.	0.001	57	71	590.	0.125
18	24	550.	0.054	58	72	595.	0.154
19	28	550.	0.048	59	73	551.	0.027
20	29	551.	0.057	60	77	550.	0.026
21	30	556.	0.100	61	78	604.	0.251
22	31	542.	0.012	62	81	543.	0.005
23	32	543.	0.011	63	82	543.	0.002
24	33	542.	0.001	64	83	589.	0.138
25	34	543.	0.010	65	84	573.	0.069
26	35	553.	0.052	66	85	569.	0.052
27	36	555.	0.066	67	86	551.	0.032
28	37	549.	0.068	68	88	567.	0.136
29	38	543.	0.013	69	89	545.	0.007
30	40	544.	0.003	70	87	546.	0.005
31	41	546.	0.011	71	91	572.	0.068
32	42	557.	0.051	72	92	549.	0.014
33	43	558.	0.058	73	93	545.	0.006
34	44	544.	0.004	74	94	544.	0.003
35	46	545.	0.012	75	95	548.	0.021
36	48	544.	0.005	76	96	544.	0.008
37	49	553.	0.052	77	97	543.	0.003
38	50	553.	0.054	78	98	543.	0.004
39	51	548.	0.034	79	99	547.	0.023
40	52	545.	0.014	80	100	542.	0.006

$\alpha = 30^{\circ}$

TEST NO. 105 RUN NO. 31

MACH	REYN/FT	REL	QS	TWSPH	PT	TT	RSPH(FT)
7.40	3.41E 06	4.58E 06	78.78	583.	759.	1423.	0.006

CHANNEL	T/C	TEMP	QW/QS	CHANNEL	T/C	TEMP	QW/QS
1	1	568.	0.293	41	54	545.	0.002
2	2	546.	0.007	42	55	556.	0.040
3	4	560.	0.170	43	56	556.	0.042
4	5	549.	0.061	44	57	547.	0.019
5	6	545.	0.018	45	58	547.	0.022
6	8	550.	0.059	46	60	545.	0.003
7	9	544.	0.003	47	61	557.	0.037
8	11	560.	0.161	48	62	557.	0.042
9	12	557.	0.137	49	63	547.	0.017
10	13	553.	0.104	50	64	611.	0.283
11	14	546.	0.038	51	65	551.	0.022
12	15	544.	0.006	52	66	546.	0.004
13	16	544.	0.005	53	67	545.	0.001
14	17	554.	0.071	54	68	545.	0.001
15	19	555.	0.077	55	69	586.	0.100
16	20	546.	0.029	56	70	577.	0.068
17	22	543.	0.001	57	71	585.	0.169
18	24	553.	0.055	58	72	586.	0.168
19	28	552.	0.047	59	73	552.	0.027
20	29	554.	0.059	60	77	555.	0.030
21	30	559.	0.101	61	78	605.	0.222
22	31	544.	0.012	62	81	546.	0.005
23	32	544.	0.010	63	82	545.	0.001
24	33	543.	0.002	64	83	597.	0.143
25	34	545.	0.012	65	84	581.	0.068
26	35	556.	0.052	66	85	579.	0.056
27	36	559.	0.065	67	86	552.	0.027
28	37	551.	0.068	68	88	569.	0.132
29	38	545.	0.013	69	89	547.	0.007
30	40	545.	0.004	70	87	549.	0.006
31	41	546.	0.010	71	91	580.	0.065
32	42	560.	0.052	72	92	553.	0.018
33	43	561.	0.059	73	93	548.	0.008
34	44	545.	0.004	74	94	547.	0.005
35	46	546.	0.013	75	95	552.	0.020
36	48	545.	0.005	76	96	547.	0.007
37	49	556.	0.051	77	97	545.	0.004
38	50	556.	0.054	78	98	546.	0.005
39	51	550.	0.042	79	99	551.	0.029
40	52	547.	0.015	80	100	546.	0.007

$\alpha = 40^{\circ}$

TEST NO. 105 RUN NO. 32

MACH	REYN/FT	REI	OS	TWSPH	PT	TT	RSPH(FT)
7.40	3.31E 06	4.45E 06	80.47	587.	755.	1446.	0.006

CHANNEL	T/C	TEMP	QW/QS	CHANNEL	T/C	TEMP	QW/QS
1	1	570.	0.340	41	54	550.	0.002
2	2	552.	0.006	42	55	565.	0.106
3	4	564.	0.178	43	56	565.	0.122
4	5	554.	0.050	44	57	550.	0.006
5	6	552.	0.011	45	58	551.	0.013
6	8	557.	0.074	46	60	550.	0.003
7	9	552.	0.003	47	61	565.	0.125
8	11	567.	0.187	48	62	566.	0.140
9	12	564.	0.153	49	63	551.	0.011
10	13	560.	0.111	50	64	592.	0.230
11	14	554.	0.033	51	65	553.	0.012
12	15	551.	0.004	52	66	550.	0.001
13	16	552.	0.006	53	67	549.	0.002
14	17	564.	0.100	54	68	549.	0.001
15	19	564.	0.096	55	69	595.	0.172
16	20	555.	0.033	56	70	597.	0.160
17	22	552.	0.000	57	71	616.	0.225
18	24	563.	0.081	58	72	619.	0.223
19	28	563.	0.072	59	73	553.	0.012
20	29	564.	0.084	60	77	557.	0.022
21	30	568.	0.126	61	78	595.	0.215
22	31	553.	0.014	62	81	550.	0.005
23	32	553.	0.012	63	82	549.	0.002
24	33	552.	0.001	64	83	610.	0.150
25	34	552.	0.005	65	84	595.	0.200
26	35	567.	0.100	66	85	617.	0.230
27	36	569.	0.114	67	86	552.	0.010
28	37	558.	0.067	68	88	569.	0.108
29	38	553.	0.014	69	89	549.	0.002
30	40	552.	0.006	70	87	551.	0.006
31	41	552.	0.005	71	91	600.	0.169
32	42	569.	0.106	72	92	556.	0.011
33	43	571.	0.142	73	93	553.	0.006
34	44	551.	0.003	74	94	551.	0.003
35	46	552.	0.013	75	95	556.	0.011
36	48	551.	0.005	76	96	552.	0.006
37	49	564.	0.110	77	97	551.	0.005
38	50	565.	0.130	78	98	552.	0.009
39	51	552.	0.020	79	99	558.	0.022
40	52	554.	0.040	80	100	551.	0.007

$\alpha = 50^{\circ}$ TEST NO. 105 RUN NO. 33

MACH	REYN/FT	REL	QS	TWSPH	PT	TT	RSPH(FT)
7.40	3.59E 06	4.82E 06	78.44	587.	785.	1410.	0.006

CHANNEL	T/C	TEMP	QW/QS	CHANNEL	T/C	TEMP	QW/QS
1	1	569.	0.360	41	54	552.	0.002
2	2	553.	0.009	42	55	575.	0.226
3	4	564.	0.184	43	56	575.	0.230
4	5	554.	0.044	44	57	552.	0.004
5	6	552.	0.007	45	58	553.	0.018
6	8	558.	0.082	46	60	552.	0.003
7	9	552.	0.004	47	61	581.	0.243
8	11	568.	0.210	48	62	581.	0.246
9	12	564.	0.169	49	63	552.	0.011
10	13	560.	0.119	50	64	583.	0.178
11	14	553.	0.031	51	65	553.	0.003
12	15	552.	0.003	52	66	553.	0.003
13	16	552.	0.006	53	67	552.	0.002
14	17	566.	0.128	54	69	552.	0.002
15	19	565.	0.112	55	69	608.	0.243
16	20	555.	0.037	56	70	602.	0.220
17	22	552.	0.001	57	71	596.	0.240
18	24	566.	0.105	58	72	600.	0.244
19	28	565.	0.086	59	73	553.	0.003
20	29	567.	0.102	60	77	562.	0.021
21	30	569.	0.141	61	78	606.	0.188
22	31	553.	0.016	62	81	554.	0.005
23	32	553.	0.014	63	82	552.	0.005
24	33	552.	0.002	64	83	624.	0.245
25	34	552.	0.007	65	84	630.	0.238
26	35	571.	0.208	66	85	621.	0.207
27	36	574.	0.220	67	86	553.	0.006
28	37	558.	0.070	68	88	568.	0.104
29	38	553.	0.016	69	89	553.	0.008
30	40	554.	0.005	70	87	551.	0.007
31	41	554.	0.006	71	91	608.	0.283
32	42	577.	0.212	72	92	555.	0.008
33	43	579.	0.228	73	93	552.	0.004
34	44	553.	0.004	74	94	551.	0.005
35	46	555.	0.019	75	95	555.	0.012
36	48	553.	0.003	76	96	552.	0.007
37	49	572.	0.220	77	97	555.	0.025
38	50	573.	0.228	78	98	558.	0.031
39	51	553.	0.012	79	99	558.	0.023
40	52	555.	0.030	80	100	552.	0.014

$\alpha = 60^{\circ}$

TEST NO. 105 RUN NO. 34

MACH	REYN/FT	PEI	QS	TWSPH	PT	TT	RSPH(FT)
7.40	7.01E 05	9.40E 05	38.47	566.	161.	1453.	0.006

CHANNEL	T/C	TEMP	QW/QS	CHANNEL	T/C	TEMP	QW/QS
1	1	557.	0.368	41	54	550.	0.003
2	2	551.	0.004	42	55	558.	0.080
3	4	555.	0.193	43	56	557.	0.086
4	5	551.	0.041	44	57	550.	0.001
5	6	550.	0.006	45	58	550.	0.007
6	8	563.	0.027	46	60	550.	0.004
7	9	550.	0.003	47	61	558.	0.074
8	11	557.	0.232	48	62	558.	0.078
9	12	556.	0.183	49	63	551.	0.002
10	13	554.	0.128	50	64	565.	0.121
11	14	551.	0.031	51	65	550.	0.002
12	15	550.	0.003	52	66	550.	0.001
13	16	551.	0.005	53	67	550.	0.002
14	17	557.	0.152	54	68	550.	0.004
15	19	556.	0.122	55	69	569.	0.130
16	20	552.	0.041	56	70	566.	0.098
17	22	550.	0.002	57	71	566.	0.081
18	24	556.	0.129	58	72	568.	0.074
19	25	556.	0.105	59	73	551.	0.003
20	29	556.	0.121	60	77	551.	0.005
21	30	557.	0.143	61	78	564.	0.101
22	31	550.	0.018	62	81	551.	0.005
23	32	550.	0.015	63	82	550.	0.003
24	33	550.	0.004	64	83	571.	0.138
25	34	550.	0.007	65	84	568.	0.090
26	35	556.	0.112	66	85	566.	0.070
27	36	557.	0.121	67	86	552.	0.009
28	37	552.	0.074	68	88	554.	0.053
29	38	550.	0.017	69	89	550.	0.002
30	40	552.	0.008	70	87	552.	0.001
31	41	552.	0.004	71	91	563.	0.106
32	42	559.	0.039	72	92	551.	0.008
33	43	560.	0.109	73	93	550.	0.004
34	44	551.	0.006	74	94	550.	0.003
35	46	551.	0.015	75	95	551.	0.008
36	48	550.	0.004	76	96	551.	0.010
37	49	557.	0.097	77	97	550.	0.006
38	50	557.	0.098	78	98	550.	0.004
39	51	550.	0.007	79	99	552.	0.022
40	52	551.	0.017	80	100	550.	0.011

$\alpha = 60^\circ$ TEST NO. 105 RUN NO. 35

MACH	REYN/FT	REL	QS	TWSPH	PT	TT	RSPH(FT)
7.40	1.45E 06	1.95E 06	52.17	577.	324.	1428.	0.006

CHANNEL	T/C	TEMP	QW/QS	CHANNEL	T/C	TEMP	QW/QS
1	1	565.	0.368	41	54	553.	0.005
2	2	554.	0.007	42	55	565.	0.082
3	4	562.	0.185	43	56	564.	0.085
4	5	555.	0.037	44	57	553.	0.003
5	6	-	-	45	58	553.	0.008
6	8	567.	0.042	46	60	554.	0.005
7	9	554.	0.002	47	61	565.	0.077
8	11	565.	0.232	48	62	565.	0.082
9	12	562.	0.184	49	63	553.	0.003
10	13	560.	0.122	50	64	576.	0.113
11	14	555.	0.027	51	65	553.	0.002
12	15	554.	0.001	52	66	553.	0.001
13	16	554.	0.004	53	67	552.	0.001
14	17	565.	0.146	54	68	552.	0.002
15	19	564.	0.123	55	69	582.	0.133
16	20	557.	0.040	56	70	577.	0.096
17	22	555.	0.001	57	71	578.	0.066
18	24	564.	0.126	58	72	580.	0.063
19	28	563.	0.107	59	73	553.	0.002
20	29	564.	0.123	60	77	552.	0.004
21	30	566.	0.141	61	78	575.	0.105
22	31	555.	0.016	62	81	549.	0.004
23	32	555.	0.016	63	82	551.	0.002
24	33	555.	0.007	64	83	583.	0.136
25	34	555.	0.005	65	84	580.	0.087
26	35	566.	0.114	66	85	577.	0.072
27	36	567.	0.116	67	86	550.	0.006
28	37	558.	0.068	68	88	557.	0.056
29	38	555.	0.015	69	89	552.	0.006
30	40	555.	0.005	70	87	550.	0.003
31	41	554.	0.004	71	91	573.	0.101
32	42	567.	0.096	72	92	557.	0.010
33	43	568.	0.107	73	93	556.	0.007
34	44	554.	0.004	74	94	555.	0.004
35	46	554.	0.015	75	95	557.	0.011
36	48	553.	0.005	76	96	557.	0.021
37	49	564.	0.094	77	97	556.	0.009
38	50	564.	0.097	78	98	554.	0.006
39	51	553.	0.007	79	99	559.	0.027
40	52	554.	0.018	80	100	557.	0.016

$\alpha = 60^\circ$

TEST NO. 105 RUN NO. 36

MACH	PEYN/FT	REI	QS	TWSPH	PT	TT	RSPH(FT)
7.40	2.54E 06	3.41E 06	62.92	586.	540.	1384.	0.006

CHANNEL	T/C	TEMP	QW/QS	CHANNEL	T/C	TEMP	QW/QS
1	1	572.	0.360	41	54	553.	0.004
2	2	556.	0.007	42	55	570.	0.084
3	4	566.	0.187	43	56	570.	0.090
4	5	557.	0.041	44	57	553.	0.003
5	6	555.	0.0	45	58	554.	0.009
6	8	559.	0.066	46	60	554.	0.002
7	9	555.	0.004	47	61	571.	0.084
8	11	570.	0.234	48	62	572.	0.088
9	12	566.	0.183	49	63	554.	0.004
10	13	562.	0.126	50	64	584.	0.132
11	14	556.	0.029	51	65	553.	0.002
12	15	554.	0.003	52	66	553.	0.001
13	16	555.	0.005	53	67	553.	0.001
14	17	569.	0.151	54	68	554.	0.002
15	19	567.	0.124	55	69	593.	0.132
16	20	557.	0.040	56	70	587.	0.099
17	22	555.	0.002	57	71	589.	0.076
18	24	568.	0.128	58	72	594.	0.084
19	28	568.	0.112	59	73	554.	0.003
20	29	569.	0.123	60	77	555.	0.004
21	30	569.	0.143	61	78	585.	0.102
22	31	555.	0.018	62	81	554.	0.005
23	32	555.	0.016	63	82	554.	0.003
24	33	554.	0.007	64	83	597.	0.135
25	34	554.	0.005	65	84	598.	0.104
26	35	570.	0.110	66	85	596.	0.102
27	36	571.	0.119	67	86	556.	0.008
28	37	559.	0.073	68	88	563.	0.063
29	38	555.	0.016	69	89	554.	0.003
30	40	554.	0.004	70	87	555.	0.006
31	41	555.	0.005	71	91	592.	0.176
32	42	573.	0.103	72	92	559.	0.009
33	43	574.	0.112	73	93	557.	0.008
34	44	554.	0.005	74	94	556.	0.005
35	46	555.	0.017	75	95	559.	0.014
36	48	554.	0.007	76	96	561.	0.024
37	49	569.	0.102	77	97	558.	0.011
38	50	570.	0.105	78	98	557.	0.009
39	51	554.	0.007	79	99	563.	0.027
40	52	555.	0.023	80	100	559.	0.023

$\alpha = 60°$

TEST NO. 105 RUN NO. 37

MACH	REYN/FT	REL	QS	TWSPH	PT	TT	RSPH(FT)
7.40	3.67E 06	4.93E 06	72.50	590.	763.	1366.	0.006

CHANNEL	T/C	TEMP	QW/QS
1	1	574.	0.352
2	2	556.	0.008
3	4	568.	0.184
4	5	557.	0.039
5	6	555.	0.0
6	8	560.	0.071
7	9	555.	0.004
8	11	573.	0.240
9	12	569.	0.190
10	13	564.	0.134
11	14	556.	0.028
12	15	555.	0.002
13	16	555.	0.005
14	17	572.	0.149
15	19	570.	0.123
16	20	558.	0.041
17	22	555.	0.002
18	24	571.	0.126
19	28	570.	0.110
20	29	572.	0.122
21	30	572.	0.142
22	31	555.	0.017
23	32	555.	0.016
24	33	555.	0.006
25	34	555.	0.007
26	35	574.	0.113
27	36	576.	0.117
28	37	561.	0.077
29	38	555.	0.016
30	40	556.	0.005
31	41	556.	0.004
32	42	579.	0.105
33	43	581.	0.113
34	44	555.	0.005
35	46	557.	0.023
36	48	555.	0.005
37	49	575.	0.109
38	50	576.	0.111
39	51	555.	0.009
40	52	558.	0.032
41	54	555.	0.003
42	55	577.	0.095
43	56	577.	0.099
44	57	555.	0.004
45	58	556.	0.011
46	60	555.	0.002
47	61	580.	0.120
48	62	580.	0.115
49	63	555.	0.003
50	64	590.	0.110
51	65	556.	0.003
52	66	555.	0.002
53	67	555.	0.002
54	68	555.	0.002
55	69	605.	0.129
56	70	598.	0.099
57	71	605.	0.088
58	72	615.	0.126
59	73	556.	0.003
60	77	-	-
61	78	594.	0.124
62	81	557.	0.006
63	82	556.	0.004
64	83	609.	0.142
65	84	622.	0.197
66	85	615.	0.166
67	86	556.	0.007
68	88	567.	0.065
69	89	556.	0.006
70	87	554.	0.007
71	91	609.	0.244
72	92	560.	0.010
73	93	558.	0.009
74	94	557.	0.007
75	95	561.	0.014
76	96	563.	0.029
77	97	559.	0.013
78	98	558.	0.011
79	99	565.	0.030
80	100	561.	0.023

$\alpha = 20^{\circ}$ TEST NO. 105 RUN NO. 38

MACH	REYN/FT	REI	QS	TWSPH	PT	TT	RSPH(FT)
7.40	3.13E 06	4.21E 06	86.36	591.	764.	1502.	0.006

CHANNEL	T/C	TEMP	QW/QS	CHANNEL	T/C	TEMP	QW/QS
1	1	577.	0.247	41	54	558.	0.006
2	2	556.	0.015	42	55	564.	0.024
3	4	560.	0.144	43	56	564.	0.026
4	5	559.	0.066	44	57	560.	0.019
5	6	557.	0.010	45	58	560.	0.019
6	8	557.	0.040	46	60	558.	0.005
7	9	553.	0.006	47	61	564.	0.021
8	11	568.	0.123	48	62	564.	0.025
9	12	566.	0.106	49	63	558.	0.014
10	13	563.	0.085	50	64	648.	0.331
11	14	557.	0.038	51	65	566.	0.026
12	15	554.	0.011	52	66	559.	0.005
13	16	554.	0.005	53	67	557.	0.001
14	17	564.	0.044	54	68	558.	0.001
15	19	566.	0.054	55	69	591.	0.090
16	20	559.	0.023	56	70	583.	0.059
17	22	556.	0.001	57	71	581.	0.056
18	24	563.	0.032	58	72	602.	0.116
19	28	563.	0.026	59	73	570.	0.037
20	29	564.	0.036	60	77	573.	0.051
21	30	571.	0.075	61	78	630.	0.264
22	31	558.	0.011	62	81	559.	0.005
23	32	558.	0.008	63	82	558.	0.001
24	33	557.	0.001	64	83	603.	0.123
25	34	559.	0.012	65	84	583.	0.056
26	35	565.	0.027	66	85	579.	0.037
27	36	568.	0.041	67	86	573.	0.053
28	37	565.	0.052	68	88	600.	0.191
29	38	559.	0.010	69	89	563.	0.014
30	40	558.	0.002	70	87	563.	0.012
31	41	560.	0.016	71	91	587.	0.074
32	42	568.	0.030	72	92	573.	0.036
33	43	570.	0.039	73	93	561.	0.011
34	44	558.	0.006	74	94	558.	0.002
35	46	559.	0.009	75	95	573.	0.051
36	48	559.	0.012	76	96	562.	0.012
37	49	564.	0.032	77	97	558.	0.005
38	50	565.	0.033	78	98	557.	0.004
39	51	560.	0.023	79	99	573.	0.099
40	52	558.	0.003	80	100	559.	0.011